Temporal fluctuation scaling in nonstationary time series using the path integral formalism

F. S. Abril [*] and C. J. Quimbay [†]
Universidad Nacional de Colombia, Departamento de Física, Bogotá, D.C., Colombia

(Received 7 December 2020; revised 25 March 2021; accepted 30 March 2021; published 15 April 2021)

We model the time evolution of the mean and the variance of nonstationary time series using the path integral formalism with the purpose to obtain the temporal fluctuation scaling presents in complex systems. To this end, we first show how the probability of change between two times of a stochastic variable can be written in terms of a Feynman kernel, where the cumulant generating function of statistical moments is identified as the Hamiltonian of the system. Thus, by including the effects of a stochastic drift and a temporal logarithmic term in the cumulant generating function, we find analytical expressions describing the temporal evolutions of the mean and the variance in terms of cumulants. Starting from these expressions, we obtain the temporal fluctuation scaling written as a general analytical relation between the variance and the mean, in such a way that this relation satisfies a power law, with the exponent being a function on time. Additionally, we study several financial time series associated with changes of prices for some stock indexes and currencies. For this financial time series, we find that the temporal evolution of the mean and the variance, the temporal fluctuation scaling, and the temporal evolution of the exponent which are obtained from this path integral approach are in agreement with those obtained using the empirical data.

DOI: 10.1103/PhysRevE.103.042126

I. INTRODUCTION

Fluctuation scaling (FS) observed in a wide variety of complex systems states the existence of a relation between the standard deviation and the mean of a probability distribution that satisfies a power law [1–3]. Two forms of this FS are essentially known: the ensemble fluctuation scaling (EFS) [1,2] and the temporal fluctuation scaling (TFS) [1,2]. An important aspect to note is that regardless of its nature (spatial or temporal), this FS is characterized by presenting itself as an emergent property of complex multifractal systems [4–7]. In fact, since its discovery by Smith in 1938 [8] and Taylor in 1961 [9], the FS has been evidenced in different areas such as ecology [10,11], complex networks [5,12], physics [4,13], financial markets [14,15], and city traffic [16]. At this point, it is worth mentioning that in the study of the TFS in financial markets, it has been found that the TFS exponent varies between $\frac{1}{2}$ and 3, and that in order to correctly analyze this type of system, it is better to take the cumulative mean into an optimal window size that also clusters the data [15]. Emphasizing the previous point, it has been found that the TFS exponent varies with time and, like the Hurst exponent, presents a logarithmic behavior in time that depends on the window size $\Delta t = t_b - t_a$ chosen for the data [17–19]. In fact, the logarithmic behavior in time of the TFS exponent, denoted by $\alpha(\Delta t)$ and strongly influenced by external factors [20], can be characterized by the increasing trend γ_t according to the type of financial market and assuming a nonuniversal value of $\alpha(\Delta t)$ [19]. In addition, the exponent $\alpha(\Delta t)$ carries the information of the properties of the collective dynamics of the entire system, and its functional form must be independent of the market and the chosen time interval Δt [19].

The main difference between EFS and TFS lies in their spatial or temporal structure, respectively, but this has not been an impediment to trying to explain its origin through statistical physics as a system in stationary or nonstationary states of equilibrium [2]. Even so, these explanations do not consider the stochastic nature that underlies the FS, and that in the temporal case many times implies nonstationary time series, where the known relation of the variance is not reflected as the difference of the second moment around the origin and the square of the mean of the distribution [21], since if this were the case, the variance would always be a quadratic function of the mean of the distribution [21]. In particular, for the stochastic variables associated with financial assets, models with nonconstant variance over time have been proposed, such as the geometric model of Brownian motion, the generalized autoregressive conditional heteroscedastic model (GARCH), the Heston model, and the nonlinear Heston model [22–24]. In these types of models, volatility is studied as a stochastic variable whose underlying dynamics is coupled to that of the financial asset through a system of stochastic differential equations in such a way that the first hitting time (FHT) characterizes the stability of the market or financial asset [22,23]. The above stochastic variable FHT is defined in a general way for any type of complex system as the characteristic time interval that a system starting from a fixed initial condition θ_i reaches a fixed final value θ_f [22–24]. In fact, it is observed that the behavior between the variance and the FHT behaves in a nonmonotonic way, reaching a maximum that sets the most optimal behavior of the system under study [25–28]. Thus, the stochastic nature of the variance does not allow us to clearly

[*] fsabrilb@unal.edu.co
[†] cjquimbayh@unal.edu.co

explain the origin of the TFS and it is necessary to introduce an approach that contains aspects such as stochastic drift and the fractal nature of the TFS to explain the causal structure of nonstationary time series [29–32].

On the other hand, the Feynman path integral is a natural description to make the evolution of two states with a causal structure in quantum mechanics [33]. Some approaches have been proposed to consider a stochastic or fractal extension of the path integral [34–38]. In the application of these approaches to systems such as financial time series (FTS), it has been shown that these have strong limitations such as the low-frequency limit in the data, the assumption of the knowledge of stochastic drift for all probability distribution, or the exponent considered in the law of invariance of fractal behavior [35–38]. Also, it is known that the Feynman kernel has a clear causal structure due to its form of construction and that in the imaginary time it provides a connection with the usual statistical physics, but this implies an evolution of the variance and upper moments of the associated probability distribution which scale linearly with time, which would not allow for decreasing trends in empirical data [39,40]. Another important fact of the path integral formalism is that the Markovian property [see Eq. (17)] describes the decomposition of the transition probability amplitude in consecutive times allowing one to characterize high peaks of time series in random times [41].

However, an approach that better describes the nature of the empirical data of nonstationary time series, and that describes the TFS, must have nonlinear terms with a stochastic drift present in each step of the calculation. For this reason, in this paper, the TFS is obtained by introducing a time-dependent logarithmic term in the cumulant generating function, which represents the Hamiltonian of the Feynman kernel in the imaginary time formalism. This approach has three fundamental aspects that are in accordance with the literature: (1) it is invariant under temporal translations and scale transformations [42]; (2) it improves the limit of high and low frequencies developed by Kleinert [35,36] and shows the stochastic drift as a minimum measure for the evolution in time of the moments of a probability distribution, that is, the minimum value that takes the moments around these origin of a distribution; and (3) it describes the temporal evolution of the TFS exponent $\alpha(\Delta t)$ independently of the market and the chosen time interval. In fact, this shows that the origin of the TFS is stochastic and nonstationary in nature, which implies that it cannot be related in principle as an equilibrium system except at a low-frequency limit where the perturbations on the system are small [2]. It is important to mention that, although all the calculations developed in this paper are limited to FTS, the formalism that follows is independent of the nature of the time series and shows the Feynman kernel as a natural tool to describe systems with causal structure, such as time series. Furthermore, the path integral approach used here leads us to estimate the variance as a deterministic variable that varies with time in contrast with the stochastic variance of the GARCH model, the Heston model, and the nonlinear Heston model.

To do the above, for the case of nonstationary time series and using the Feynman path integral formalism, we show how the probability of change between two times of a stochastic variable can be written in terms of a Feynman kernel, where the cumulant generating function of statistical moments is identified as the Hamiltonian of the system. Next, we include the effects of a stochastic drift and a cumulant generating function with a temporal logarithmic term, and we find analytical expressions that describe the temporal evolutions of the mean and the variance in terms of cumulants. With these expressions, we obtain the TFS as a general analytical relation that describes the variance as a function of the mean, in such a way that this relation satisfies a power law, with the exponent being a function on time. Finally, with the purpose of validating this approach, we study the time series of log-returns, volatilities, and absolute values of log-returns for the following four stock indexes: Nikkei 225 (Japan, daily frequency), S&P 500 (United States, daily frequency), Dow Jones (United States, frequency every 2 sec) and FTSE (England, daily frequency), and for the following currency: the Colombian peso to U.S. dollar exchange rate (COP-USD). We find for these financial time series that the temporal evolutions of the mean and the variance obtained from the analytical expressions are in agreement with those obtained from the empirical data. We find also that the TFS obtained by using this path integral approach is consistent with the one obtained from the empirical data. Specifically, we find agreement between the temporal evolutions of the TFS exponent obtained using the analytical expression and the empirical data. It is important to mention that high- and low-frequency time series are studied to see that the proposed fit is independent of the frequency of the data and is totally determined by a scale parameter b defined with a time-dependent logarithmic term [see Eq. (31)]. Furthermore, the study of low-frequency data (daily data) is important in the study of financial markets since it allows one to speculate in a more distant future about the behavior that a financial asset may follow even when its description seems to be more difficult and is nondeterministic.

The structure of this paper is as follows: in Sec. II we define the nonstationary time series and the cumulant generating function. In Sec. III the Feynman path integral is established in the imaginary time formalism that together with the evolution equation of a financial asset defined in Sec. III A allows us to establish the evolution in time of a probability distribution related to a financial derivative in the Kleinert model [35,36]. In Sec. III B the evolution in time of the moments of the probability distribution is mentioned adding the effect of the stochastic drift. Then, taking into account the problems of Kleinert model and the TFS, in Sec. IV the generalization of the TFS is made by including a temporal logarithmic term in the cumulant generating function that accounts for the low-frequency limit. In Sec. V we define the time series of log-returns of prices, volatilities, and the absolute value of log-returns for each stock index which are distributed as a truncated Lévy flight distribution, a two-parameter Gamma distribution, and a distribution of a Boltzmann (Laplace distribution), respectively. From these FTS, the evolution of the first moment (mean) is studied in three different ways. Additionally, in Sec. V D we study the evolution over time of the mean and the variance of COP-USD currency, allowing us to estimate the highest value of this time series with good precision and accuracy, once the associated financial asset is known for the previous time period. Finally, in Sec. VI we

study the time evolution of the TFS exponent for the five FTS considered. In Sec. VII we present conclusions, and some topics towards which the investigation is still directed are laid out. Finally, in Appendix A we show the analytical deduction of the evolution in time of the moments of a probability distribution of a financial derivative using the formula of Faà di Bruno. In Appendix B, the temporal evolution of the probability distribution is calculated using a nonzero stochastic drift since it is often not trivial to recognize the value of the stochastic drift from the empirical data. In Appendix C we present the deduction of the mean and the variance as functions of time for a probability distribution, by including a weighting function in the calculation of the moments of the distribution. It is important to mention that this weighting function is what allows us to talk about the previously defined time-dependent logarithmic term. In Appendix D we show the regression data obtained for each stock index. In Appendix E we show the verification of Markov property for each financial asset.

II. CUMULANT GENERATING FUNCTION AND NONSTATIONARY TIME SERIES

In general, a time series corresponds to the realization of a discrete stochastic process X_t with $t \in \mathbb{N}$. The weak-sense stationarity or wide-sense stationarity (WSS) of a discrete stochastic process X_t is defined as a random process in which the mean $\mathbb{E}[X_t] \equiv m_X(t)$ and autocovariance function $\mathbb{E}[[X_{t_1} - m_X(t_1)][X_{t_2} - m_X(t_2)]] \equiv K_{XX}(t_1, t_2)$ do not vary in time [21]:

$$\mathbb{E}[X_t] = \mathbb{E}[x(t+\tau)], \quad \text{for all } \tau \in \mathbb{N}, \tag{1}$$

$$K_{XX}(t_1, t_2) = K_{XX}(t_1 - t_2, 0), \quad \text{for all } t_1, t_2 \in \mathbb{N}, \tag{2}$$

$$\mathbb{E}[|X_t|^2] < \infty, \quad \text{for all } t \in \mathbb{N}. \tag{3}$$

A time series is nonstationary if the above definition is not satisfied. Henceforth, it is assumed that the time series are nonstationary, and for simplicity, from now on we will refer to time series as nonstationary time series.

Let $\widetilde{D}(z)$ be an arbitrary probability density function such that $\int_{\mathbb{R}} \widetilde{D}(z)\, dz = 1$. For this arbitrary probability distribution function $\widetilde{D}(z)$, its decomposition in Fourier modes is defined as [36]

$$\widetilde{D}(z) = \int_{\mathbb{R}} \frac{dp}{2\pi} e^{ipz} e^{-H(p)} = \int_{\mathbb{R}} \frac{dp}{2\pi} e^{ipz} D(p), \tag{4}$$

where $D(p)$ are the Fourier components that are established to relate to the cumulant generating function $H(p)$ (also called the second characteristic function) as $D(p) = e^{-H(p)}$. Furthermore, since the characteristic function $\varphi(p)$ is defined as the Fourier transform of $\widetilde{D}(z)$, an equivalent definition for the cumulant generating function is $D(p) = e^{-H(p)} = \mathbb{E}[e^{-ipz}] = \varphi(p)$ [43]. This establishes the relationship of the cumulant generating function with the probability distributions through the characteristic function. The moments around the origin of distribution will be given by the characteristic function $\varphi(p)$ since for all $n \in \mathbb{N}$, it has

$$\mathbb{E}[z^n] \equiv \mu_n = \int_{\mathbb{R}} z^n\, \widetilde{D}(z)\, dz = i^n \frac{d^n}{dp^n} e^{-H(p)} \bigg|_{p=0}. \tag{5}$$

In the case where the cumulant generating function is an analytical function,

$$H(p) = -\ln[\mathbb{E}[e^{-ipz}]] = -\sum_{n=1}^{\infty} c_n \frac{(-ip)^n}{n!}, \tag{6}$$

it is found that the moments around the origin μ_n can be expressed as

$$\mu_n = i^n \sum_{k=1}^{n} \mathcal{B}_{n,k}((-i)c_1, \ldots, (-i)^{n-k+1} c_{n-k+1}), \tag{7}$$

where $\mathcal{B}_{n,k}$ are called Bell's incomplete polynomials [44,45] and $c_n = -i^n H^{(n)}(0)$ are the cumulants of the probability density function corresponding to the coefficients of the cumulant generating function power series. The inverse relation, that is, the cumulants c_n, in a function of moments around the origin μ_n and the expressions in the case of the central moments $\mathbb{E}[(z - \mu_1)^n] \equiv \xi_n$ are

$$c_n = i^n \sum_{k=1}^{n} (-1)^{k-1} (k-1)! \mathcal{B}_{n,k} \times ((-i)\mu_1, ..., (-i)^{n-k+1} \mu_{n-k+1}), \tag{8}$$

$$\xi_n = i^n \sum_{k=1}^{n} \mathcal{B}_{n,k}(0, ..., (-i)^{n-k+1} c_{n-k+1}), \tag{9}$$

$$c_n = i^n \sum_{k=1}^{n} (-1)^{k-1} (k-1)! \mathcal{B}_{n,k}(0, ..., (-i)^{n-k+1} \xi_{n-k+1}), \tag{10}$$

respectively. It is important to mention that the above expressions are deduced using the Faà di Bruno formula [46] and is found in Appendix A.

Finally, in order to be able to make a comparison of the statement in Eq. (9), the first four complete exponential Bell polynomials are calculated [44,45]:

$$\mathcal{B}_1(c_1) = c_1, \tag{11}$$

$$\mathcal{B}_2(c_1, c_2) = c_1^2 + c_2, \tag{12}$$

$$\mathcal{B}_3(c_1, c_2, c_3) = c_1^3 + 3c_1 c_2 + c_3, \tag{13}$$

$$\mathcal{B}_4(c_1, c_2, c_3, c_4) = c_1^4 + 3c_2^2 + 6c_1^2 c_2 + 4c_1 c_3 + c_4. \tag{14}$$

III. FEYNMAN KERNEL FOR NONSTATIONARY TIME SERIES

In the functional formalism, Feynman's kernel or amplitude of transition probability from a state at position x_a in the time t_a to a state at position x_b in the time time t_b, is defined as [33]

$$\mathcal{K}(x_b, t_b; x_a, t_a) = \int \mathcal{D}x \int \frac{\mathcal{D}p}{2\pi} e^{-\frac{i}{\hbar} S(x, \dot{x}, p)} = \int \mathcal{D}x \int \frac{\mathcal{D}p}{2\pi} e^{-\frac{i}{\hbar} \int_{t_a}^{t_b} dt \{p(t)\dot{x}(t) - H[p(t), x(t)]\}}, \tag{15}$$

where $\mathcal{D}x$ and $\mathcal{D}p$ correspond to functional measures in the space of positions and moments, respectively [47–49], and

$S(x, \dot{x}, p)$ correspond to the classical action of the system [50]. This amplitude of transition is the result of interference between the possible paths in the configuration space, each contributing a weight proportional to the exponential of its classical action. All possible paths will contribute to the integral, but their contribution will be more significant the closer the path of the classical trajectory is found [33].

In the imaginary time formalism and taking units as natural ($\hbar = 1$), the Feynman kernel is

$$\mathcal{K}(x_b, \beta; x_a, 0) = \int \mathcal{D}x \int \frac{\mathcal{D}p}{2\pi} e^{\int_0^\beta d\tau \{ip(\tau)\dot{x}(\tau) - H[p(\tau), x(\tau)]\}}. \quad (16)$$

We observe that Eq. (16) has the same structure as an inverse Fourier transform by which the Hamiltonian is related to the cumulant generating function [34–36]. Also, it is observed that with the same analogy, there is an effective Lagrangian system $\mathcal{L}(x(\tau), \dot{x}(\tau))$ corresponding to $\mathcal{L}(x(\tau), \dot{x}(\tau)) = ip(\tau)\dot{x}(\tau) - H(p(\tau), x(\tau))$.

An important property to highlight of the Feynman kernel is its semigroup property [33,34]; that is, the transition probability amplitude between times $t_a < t_b < t_c$ is given by

$$\mathcal{K}(x_c, t_c; x_a, t_a) = \mathcal{K}(x_c, t_c; x_b, t_b)\mathcal{K}(x_b, t_b; x_a, t_a), \quad (17)$$

where x_a, x_b, and x_c are the positions corresponding to each time. This property indicates that the amplitude of the transition probability is cumulative, that is, it adds up over all the positions and times between two points in space-time. Thus, the path integral is a natural formalism to describe processes that are cumulative in time. At this point it is worth mentioning that the semigroup property also defines a Markovian structure on the path integral that has been verified with empirical data to be able to reconstruct the stochastic evolution equations [41].

A. Connection between Feynman path integral and time series

The stochastic differential equation that defines the change of an instrument, asset, or financial derivative x in the Kleinert model is given by [32,34]

$$\dot{x} = r_x + \eta(t), \quad (18)$$

where r_x is called *stochastic drift* and indicates how the average value of the change of the instrument, asset, or financial derivative evolves over time, that is, $\mathbb{E}[x(t)] = r_x$. The term $\eta(t)$ corresponds to a random variable that is distributed with an arbitrary distribution at each instant of time t. This indicates the separation of the evolution of $x(t)$ into a deterministic part associated with stochastic drift r_x and a stochastic part associated with noise $\eta(t)$. It is worth noting that generally $x(t) = \ln[S(t)]$ corresponds to the log-return of the stock or financial asset and corresponds to one of the time series analyzed in Sec. V.

It is important to mention that unlike Kleinert [35,36], the stochastic drift is maintained in all the calculations since in contrasting the model with the empirical data, it is not always easy to remove the value of the stochastic drift from the data. Furthermore, knowing the stochastic drift of the distribution implies knowing the adjustment parameters of a probability distribution, which is not always trivial to calculate. An example of the above is the log-returns time series that is distributed as a series of truncated Lévy flights [35], whose parameters are difficult to adjust due to their thick tails.

The evolution of the probability that the system takes the value x_b in the time t_b since it had the value x_a in the time t_a has a probability distribution given by [34,35,38]

$$P(x_b, t_b|x_a, t_a) = \int \frac{dp}{2\pi} e^{ip(x_b - x_a) - (t_b - t_a)H(p)}, \quad (19)$$

where $t \equiv t_b - t_a = \Delta t$ is the time interval of a time series ordered temporarily and $x \equiv x_b - x_a$ is the range of values it takes in the future the instrument, asset, or financial derivative. For simplicity, by adopting the above notation and assuming that $r_x \neq 0$, the probability distribution over time has to be (see Appendix B)

$$P(x, t) = \int \frac{dp}{2\pi} e^{ipx - ipr_x - tH(p)}. \quad (20)$$

It is important to note that Eq. (20) is useful for any type of distribution, and although it provides the probability distribution of an instrument, asset, or financial derivative in a future time, it does so for discrete times, that is, for times measured in integer intervals with respect to $t \equiv t_b - t_a$.

B. Evolution of distribution moments associated with time series

Starting from Eq. (20) and taking the stochastic drift $r_x = 0$, the moments are defined as a function of time as

$$\mathbb{E}[x^n(t)] = \int_{-\infty}^{\infty} dx x^n P(x, t) = \int_{-\infty}^{\infty} \frac{dp}{2\pi} e^{-tH(p)} \int_{-\infty}^{\infty} (-i)^n \frac{\partial^n}{\partial p^n} e^{ipx}\, dx. \quad (21)$$

Remembering the representation of the Dirac δ and taking out the operator derivation from the integral, then

$$\mathbb{E}[x^n(t)] = \int_{-\infty}^{\infty} dp\, e^{-tH(p)} (-i)^n \frac{d^n}{dp^n} \delta(p). \quad (22)$$

After n partial integrations, we have

$$\Upsilon_n(t) \equiv \mathbb{E}[x^n(t)] = i^n \left[\frac{d^n}{dp^n} e^{-tH(p)} \right]_{p=0}. \quad (23)$$

For the evaluation of this derivative, an analogy is made with the development made in Appendix A with $f(p) = e^p$, $g(p) = -tH(p)$ and Eqs. (A5) and (A4). We obtain

$$\Theta_n(t) \equiv c_n(t) = -ti^n H^{(n)}(0) = tc_n, \quad (24)$$

$$\Upsilon_n(t) \equiv \mu_n(t) = i^n \sum_{k=1}^{n} \mathcal{B}_{n,k}((-i)\Theta_1(t), (-i)^2\Theta_2(t), \ldots, (-i)^{n-k+1}\Theta_{n-k+1}(t)), \quad (25)$$

$$\Xi_n(t) \equiv \xi_n(t) = i^n \sum_{k=1}^{n} \mathcal{B}_{n,k}(0, (-i)^2\Theta_2(t), \ldots, (-i)^{n-k+1}\Theta_{n-k+1}(t)), \tag{26}$$

$$\Theta_n(t) \equiv c_n(t) = i^n \sum_{k=1}^{n} (-1)^{k-1}(k-1)!\mathcal{B}_{n,k}((-i)\Upsilon_1(t), \ldots, (-i)^{n-k+1}\Upsilon_{n-k+1}(t)), \tag{27}$$

$$\Theta_n(t) \equiv c_n(t) = i^n \sum_{k=1}^{n} (-1)^{k-1}(k-1)!\mathcal{B}_{n,k}(0, (-i)^2\Xi_2(t), \ldots, (-i)^{n-k+1}\Upsilon_{n-k+1}(t)). \tag{28}$$

Equations (24), (25), (26), (27), and (28) describe the temporal evolution of the cumulants from the initial cumulants, the temporal evolution of the moments around the origin in time t based on the cumulants at that same moment of time, the temporal evolution of the moments around the mean in time t based on the cumulants at that same moment of time, the temporal evolution of the cumulants in time t based on the moments around the origin at that same moment of time, and the temporal evolution of the cumulants in time t based on the moments around the mean at that same moment of time. It is important to mention that each cumulant grows linearly over time.

Stochastic drift is included when taking the minimal substitution defined by $c_1 t \to c_1' t = c_1 t + r_x$. Finally, the standardized cumulants regarding variance are

$$N_n^{(r_x)}(t) = \frac{\Theta_n^{(r_x)}(t)}{\left[\Theta_2^{(r_x)}(t)\right]^{\frac{n}{2}}} = \frac{tc_n + \delta_{1,n}(-i)r_x}{t^{\frac{n}{2}}c_2^{\frac{n}{2}}} = t^{1-\frac{n}{2}}\bar{c}_n - i\delta_{1,n}t^{-\frac{n}{2}}\frac{r_x}{c_2^{\frac{n}{2}}}, \tag{29}$$

where $\delta_{i,j}$ is the Kronecker delta. It is observed that when the variance of the distribution c_2 exists, then when increasing the time interval t, the standardized cumulants tend to zero for $n \geqslant 3$, corroborating the central limit theorem in the version of quantum statistical physics [21,34,51].

It is important to note that in the case where the stochastic drift is introduced, all the cumulants acquire a shift in r_x, that is, the evolution of the moments $\Upsilon_n(t)$ around the origin acquires a different form, although the correlation functions remain invariant since the latter correspond to fixed filter processes. Thus, another interpretation of the stochastic drift is assigned as a parameter of the formalism that scales the evolution of all the moments around the origin to a minimum value r_x. Table I provides this new relationship for the first four central moments $\Xi_n^{(r_x)}(t)$ and $\Upsilon_n^{(r_x)}(t)$ around the origin.

TABLE I. Relationship for the first four central moments $\Xi_n^{(r_x)}(t)$ and $\Upsilon_n^{(r_x)}(t)$ around the origin based on the cumulants $\Theta_n^{(r_x)}(t)$ including the stochastic drift of the process of Eq. (18).

Order	$\Upsilon_n^{(r_x)}(t)$	$\Xi_n^{(r_x)}(t)$
1	$tc_1 + r_x$	0
2	$(tc_1 + r_x)^2 + tc_2$	tc_2
3	$(tc_1 + r_x)^3 + 3t(tc_1 + r_x)c_2 + tc_3$	tc_3
4	$(tc_1 + r_x)^4 + 3t^2c_2^2 + 6t(tc_1 + r_x)^2c_2 + 4t(tc_1 + r_x)c_3 + tc_4$	$3t^2c_2^2 + tc_4$

It is important to note that the inclusion of the stochastic drift does not modify the central moments of the distribution $\Xi_n(t)|_{r_x \equiv 0} = \Xi_n^{(r_x)}(t)$, which implies an invariance of the evolution of the moments around the mean under stochastic drift.

Note that the above expressions do not satisfy Eq. (1), which implies that Feynman path integral formalism is a natural formulation for time series because of its orderly causal structure.

It is clear that the variance as a function of the mean would always imply a quadratic dependence since

$$\Xi_2^{(r_x)}(t) = tc_2 = \Upsilon_2^{(r_x)}(t) - (tc_1 + r_x)^2 = \Upsilon_2^{(r_x)}(t) - \left[\Upsilon_1^{(r_x)}(t)\right]^2. \tag{30}$$

This restricts the behavior of the variance as a function of the mean to a polynomial form that does not reflect the FS, present in complex systems [1–3].

IV. THEORETICAL APPROACH OF TFS THROUGH TIME-DEPENDENT LOGARITHMIC TERM

In order to extend the evolution of the distribution associated with the time series to satisfy the TFS, better describe the empirical low-frequency data, and improve the fit of the data with the theory, is necessary including in the cumulant generating function a logarithmic term defined as

$$H_{ln}(p, t) = ipb\,\frac{\ln(1+t)}{t}, \tag{31}$$

where $b \in \mathbb{R}$ is a scale parameter even when it achieves negative values. It is important to mention that this logarithmic term is motivated by the evidence of a logarithmic trend in time of the Hurst exponent and the variation of the TFS exponent [17–19]. In general, the cumulant generating function can be thought as a Hamiltonian in the path integral imaginary time formalism, which implies that the classical dynamics of the real part is not altered. However, the dynamics with the new term allows the moments to scale more slowly since $\ln(1+t) = O(t)$. Thus, using a reasoning analogous to Eq. (21), the mean and variance of the distribution evolve through the following expressions [see Appendix C, Eq. (C4), and Eq. (C5)]

$$\Upsilon_1^{(H)}(t) = r_x + c_1 t + b\ln(1+t) = \Upsilon_1^{(r_x)} + b\ln(1+t), \tag{32}$$

$$\Xi_2^{(H)}(t) = c_2 t - c_1 bt\ln(1+t) - r_x b\ln(1+t) - b^2\ln^2(1+t), \tag{33}$$

respectively, where the super index H refers to the new temporal evolution with time-dependent logarithmic term [see Eq. (31)]. It is important to mention that for the adjustment of normalized higher order moments such as skewness and kurtosis, they are not considered to be fairly complex nonlinear regression models. Finally, solving for the term $b\ln(1+t)$ in Eq. (32) and replacing it in Eq. (33) it is obtained that the variance as a function of the mean is

$$\begin{aligned}\Xi_2^{(H)}(t) &= c_2 t - (c_1 t + r_x + b\ln(1+t))b\ln(1+t)\\ &= c_2 t - \left[\Upsilon_1^{(H)}(t) - r_x - c_1 t\right]\Upsilon_1^{(H)}(t)\\ &= c_2 t + (c_1 t + r_x)\Upsilon_1^{(H)}(t) - \left[\Upsilon_1^{(H)}(t)\right]^2\\ &= \Xi_2^{(r_x)}(t) + \Upsilon_1^{(r_x)}(t)\Upsilon_1^{(H)}(t) - \left[\Upsilon_1^{(H)}(t)\right]^2. \end{aligned} \tag{34}$$

Equation (34) shows that the variance has a linear and quadratic dependence with respect to the mean, which allows us to establish in a first approximation the behavior of the TFS [1–3] as will be seen in Sec. VI. It is clear that if $c_1 t + r_x \ll 1$, then the dominant term in Eq. (34) is the quadratic term, which implies a nonlinear behavior between mean and variance. Thus, from now on we refer to this as the TFS (we will show the reason of this name below), such that if $b = 0$, it reduces to the known case of Eq. (30).

In conclusion, the inclusion of this dependent logarithmic term (31) has the properties that (1) for small times (high frequency) it tends to be constant, (2) asymptotically it behaves linearly, and (3) it better reproduces the behavior of the TFS.

On the other hand, it can be thought that the relationship between the variance as a function of the mean is nonlinear, which leads to TFS [1–3]. In this case, we propose the following ansatz:

$$\Xi_2^{(H)}(t) = K\left[\Upsilon_1^{(H)}(t)\right]^{\alpha(t)}, \tag{35}$$

with $K > 0$. Now notice that we assume that the exponent of the ansatz (35) varies with time, and then it should be through the generalized TFS, which arises naturally from Feynman's description path integral with logarithmic term [see Eq. (31) and Eq. (34)]. Hence, equaling the logarithm of Eq. (33) with the logarithm of the ansatz equation (35) for time series with positive values, we obtain

$$\begin{aligned}\alpha(t) &= \frac{\ln\left[\Xi_2^{(H)}(t)\right]}{\ln\left[K\Upsilon_1^{(H)}(t)\right]}\\ &= \frac{1}{\ln\left[K\Upsilon_1^{(H)}(t)\right]}\{\ln[c_2 t - c_1 bt\ln(1+t)\\ &\quad - r_x b\ln(1+t) - b^2\ln^2(1+t)]\}. \end{aligned} \tag{36}$$

In the following sections we verify that the ansatz proposed in Eq. (35) behaves well with respect to the empirical data, highlighting the three properties that this new term [see Eq. (31)] enjoys in the cumulant generating function.

V. PROVING THE VALIDITY OF THE APPROACH IN FTS

To establish the independence of the adjustment of Eq. (32), the adjustment of the mean of the low-frequency time series (S&P 500, Nikkei 225, FTSE), and the high-frequency time series (Dow Jones), is done in three ways: taking all the data from the time series, taking the scaled data (taking every n data), and taking the temporarily moved data. It is important to mention that due to the amount of data in the time series of the Dow Jones index, only the filtered time series was taken every 20 data (every 40 sec) and temporarily transferred 220 000 data (approximately nine days), due to the high computing time. For this reason, in Appendix D there is no regression data for the time series of the Dow Jones stock index taking the total data. From this, three time series are defined with the closing price of the stock index S_i given by the log-return LR, volatility LV, and absolute log-return LA:

$$LR_i = \ln(S_{i+1}) - \ln(S_i), \tag{37}$$

$$LV_i = \frac{1}{\max_{1\leqslant k\leqslant N}|LR_k|}\sqrt{\left|\frac{LR_i - \mathbb{E}[LR]}{\sigma(LR)}\right|}, \tag{38}$$

$$LA_i = |LR_i|, \tag{39}$$

respectively. The subindex refers to the data of interest, N is the total number of data, $\mathbb{E}[\cdot]$ is the expectation value, and $\sigma(\cdot)$ is the standard deviation. It is important to mention that these three time series are those considered by Kleinert in his work, and that due to the semigroup property of the path integral, it is immediate to consider the statistical moments of the accumulation of the data by time windows and not a moving window through the time series. For this same reason, a criterion of the Markovian property [41] is also established through a χ^2 test of goodness of fit. These results are placed in Appendix E and indicate that in most cases the time series considered satisfy the Markovian property quite well by having a high P value even when the number of degrees of freedom with which the values are adjusted to a binomial distribution is high in most cases. Note in Table VI that the currency is the FTS with the smallest P values and highest χ^2 indicating that it is the one that satisfies the Markovian property criterion with the least probability assuming as the null hypothesis that the data satisfy the Markov property.

A measure of the quality of the adjustments is determined with the χ^2 test of the mean and variance and the global average error (GBE) of the mean and variance defined by

$$\chi^2_{\Upsilon_1} = \sum_{k=1}^{N/WS}\frac{|M_k(WS) - \Upsilon_1(k)|^2}{\Upsilon_1(k)}, \tag{40}$$

$$\chi^2_{\Xi_2} = \sum_{k=1}^{N/WS}\frac{|V_k(WS) - \Xi_2(k)|^2}{\Xi_2(k)}, \tag{41}$$

$$GBE_{\Upsilon_1}(\%) = \frac{WS}{N}\sum_{k=1}^{N/WS}\frac{|M_k(WS) - \Upsilon_1(k)|}{|\Upsilon_1(k)|}\times 100\%, \tag{42}$$

$$GBE_{\Xi_2}(\%) = \frac{WS}{N}\sum_{k=1}^{N/WS}\frac{|V_k(WS) - \Xi_2(k)|}{|\Xi_2(k)|}\times 100\%, \tag{43}$$

respectively. In expressions (40), (41), (42), and (43), given a temporary window size WS, $\Upsilon_1(k)$, and $\Xi_2(k)$ denote the theoretical value of the adjustment made with Eqs. (32) and (33) knowing the model parameters; $M_k(WS)$ and $V_k(WS)$

TABLE II. Regression data used to calculate the evolution of the mean and variance over time for foreign exchange COP-USD measured daily from July 16, 2010 to February 11, 2020. Theoretical data are extracted from the Kleinert model [35,36].

Time series	COP-USD Log-return	COP-USD Volatility	COP-USD Abs Log-return	COP-USD Log-return	COP-USD Volatility	COP-USD Abs Log-return
Filtration	Mean	Mean	Mean	Variance	Variance	Variance
Cumulant 1 regression c_1	2.750×10^{-7}	5.458×10^{-6}	1.302×10^{-6}	-9.419×10^{-5}	-8.404×10^{-5}	-8.984×10^{-5}
Cumulant 2 regression c_2	–	–	–	1.981×10^{-5}	2.112×10^{-5}	1.775×10^{-5}
Drift regression r_x	4.222×10^{-3}	6.843×10^{-2}	3.913×10^{-2}	-1.243×10^{-1}	-1.554×10^{-1}	-1.177×10^{-1}
b	-6.530×10^{-4}	-7.966×10^{-3}	-4.667×10^{-3}	2.191×10^{-2}	2.557×10^{-2}	2.063×10^{-2}
Drift theory r_x	1.257×10^{-3}	3.288×10^{-2}	-1.366×10^{-3}	9.354×10^{-3}	2.831×10^{-2}	-1.385×10^{-3}
Cumulant 1 theory c_1	1.140×10^{-6}	3.590×10^{-2}	1.645×10^{-2}	5.161×10^{-3}	3.080×10^{-2}	1.670×10^{-2}
Cumulant 2 Theory c2	–	–	–	3.045×10^{-3}	5.135×10^{-3}	2.768×10^{-3}
χ^2	4.035×10^{-2}	8.621×10^{-1}	7.270×10^{-1}	1.503×10^{-2}	1.463×10^{-1}	7.616×10^{-2}
Global error GBE (%)	27.19	7.93	7.51	8.61	5.65	7.02
Optimal window	20	2	2	132	132	132

denote the mean and variance of the sample of $WS * k$ accumulated data for any of the three time series (37), (38), and (39), respectively.

It is important to mention that the time series of log-returns is distributed as a truncated Lévy flight distribution [40,52], the series of volatilities as a Gamma distribution of two parameters [36], and the time series of absolute log-returns as a Laplace distribution (double exponential) [35,53,54].

For all the regressions carried out, the linear Kleinert model and the new logarithmic term were taken into account. In addition, for a better correspondence between the empirical data and the (32), it is necessary to calculate an optimal window size corresponding to the time window that minimizes the error of the parameters (b, r_x, c_1) with respect to the final data. Also, the χ^2 test and the GBE (%) for each time series are also calculated and placed in Tables II and VI.

A. Evolution of total time series

In this first method with the total data of each time series, Figs. 1, 2, and 3 are obtained for the Nikkei 225, S&P 500, and FTSE index, respectively. To obtain the empirical data from the graph, the average of the total accumulated data in each window was taken; that is, if WS is the window size that optimizes the adjustment, then the average is taken every WS datum, $2WS$ datum, and so on. It is observed that the regression with logarithmic term better adjusts the trend of the empirical data and that unlike the Kleinert model it takes into account possible falls or steep increases in the index value. Furthermore, regardless of the FTS, it is observed that the adjustment to Eq. (32) follows the trend of the empirical data; however, in the case of the log-returns there is a high global average error according to Table V.

B. Evolution of scaled time series

In this method with the scaling of the data of each time series, Figs. 4, 5, 6, and 7 are obtained for the Nikkei 225, S&P 500, Dow Jones, and FTSE stock index, respectively. These figures allow us to deduce that the regression with logarithmic term better adjusts the tendency of the empirical data and that in addition to comparing with the previous method the form of the regression curve prevails with (32), which implies that the adjustment with the logarithmic term is invariant under scaling which does not occur with the Kleinert model. Here again a high degree of GBE is observed for the time series of log-return even when the χ^2 test is much less than 1 as shown in Table V. Also, it is observed in Fig. 6 the linear approximation to describe the empirical data set is not good

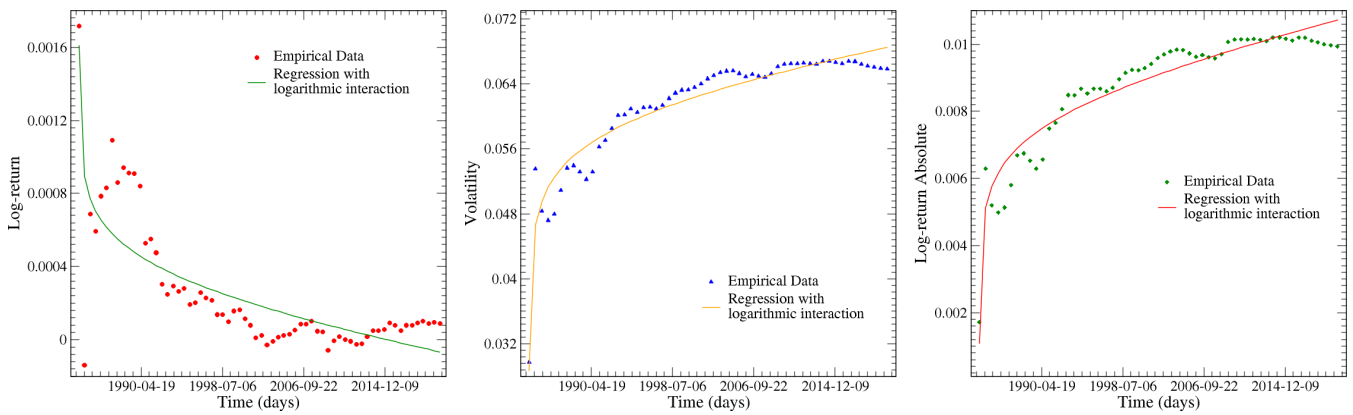

FIG. 1. Evolution of the mean of the time series of the Nikkei 225 stock index measured daily from January 4, 1984 to August 24, 2020 taking the average of the total accumulated data each window size WS. Left: Log-return time series ($WS = 138$ data). Center: Volatility time series ($WS = 159$ data). Right: Log-return absolute time series ($WS = 159$ data).

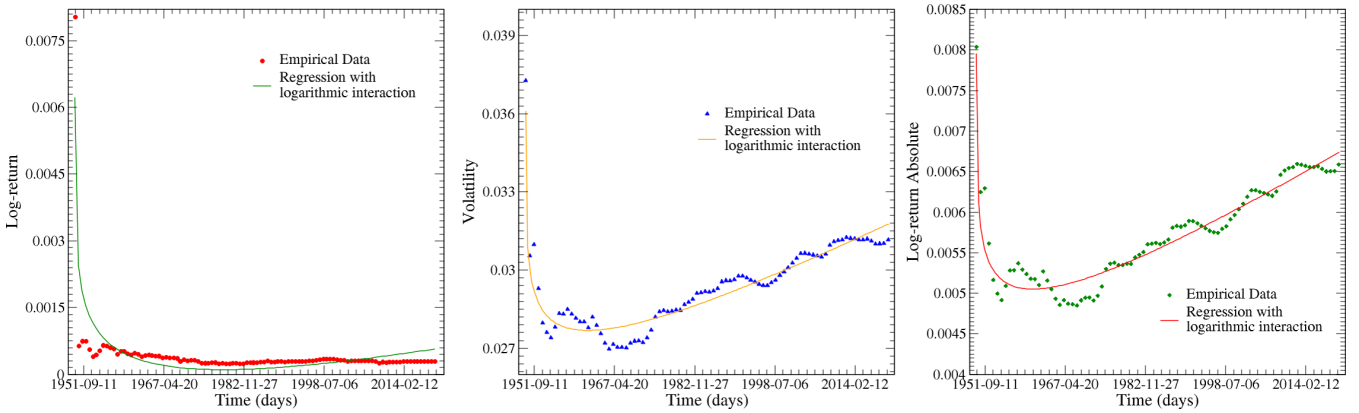

FIG. 2. Evolution of the mean of the time series of the S&P 500 stock index measured daily from January 3, 1950 to August 24, 2020 taking the average of the total accumulated data each window size WS. Left: Log-return time series ($WS = 171$ data). Center: Volatility time series ($WS = 102$ data). Right: Log-return absolute time series ($WS = 102$ data).

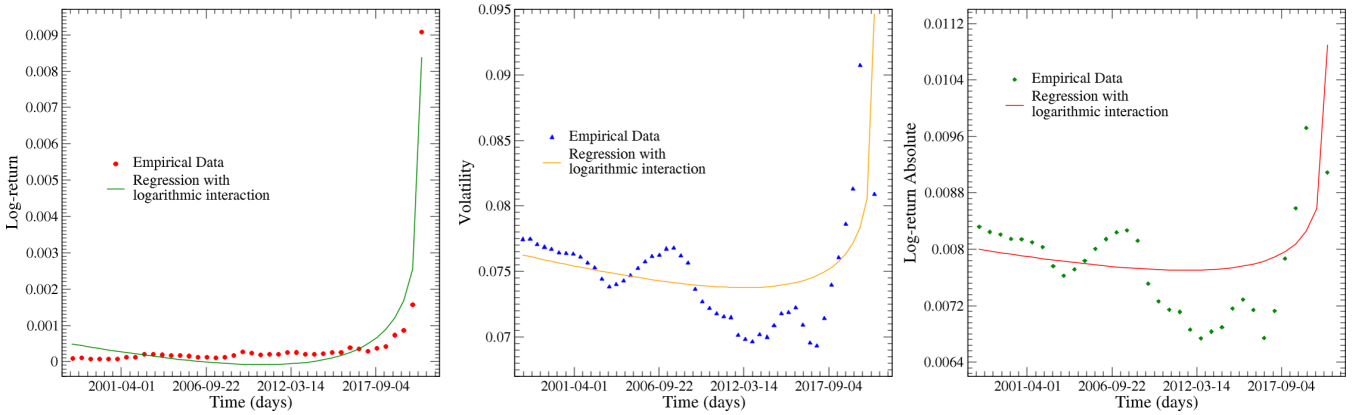

FIG. 3. Evolution of the mean of the time series of the FTSE stock index measured daily from October 20, 1997 to August 24, 2020 taking the average of the total accumulated data each window size WS. Left: Log-return time series ($WS = 146$ data). Center: Volatility time series ($WS = 117$ data). Right: Log-return absolute time series ($WS = 172$ data).

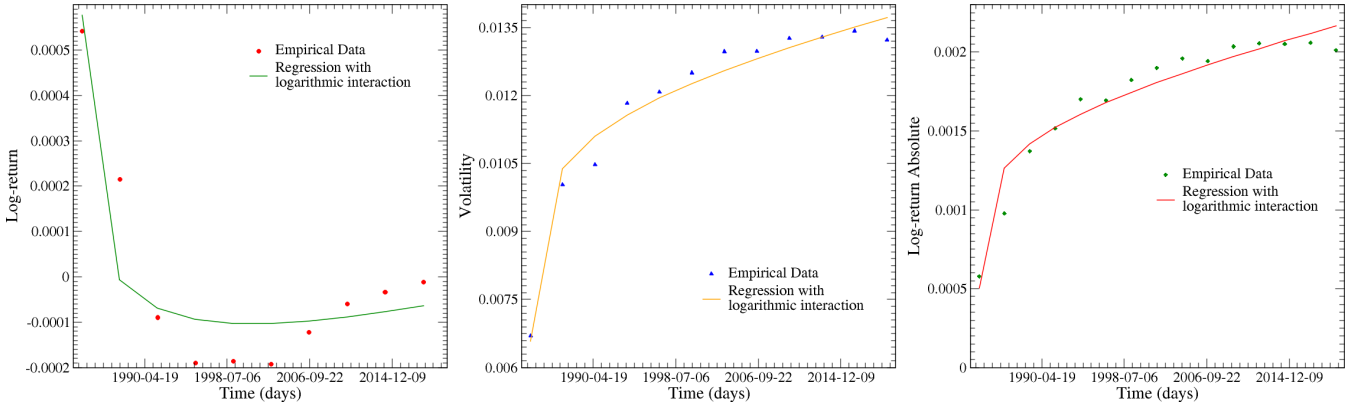

FIG. 4. Evolution of the mean of the time series of the Nikkei 225 stock index measured daily from January 4, 1984 to August 24, 2020 by scaling the data weekly (every five data) and taking the average of the total accumulated data each window size WS. Left: Log-return time series ($WS = 186$ data). Center: Volatility time series ($WS = 159$ data). Right: Log-return absolute time series ($WS = 125$ data).

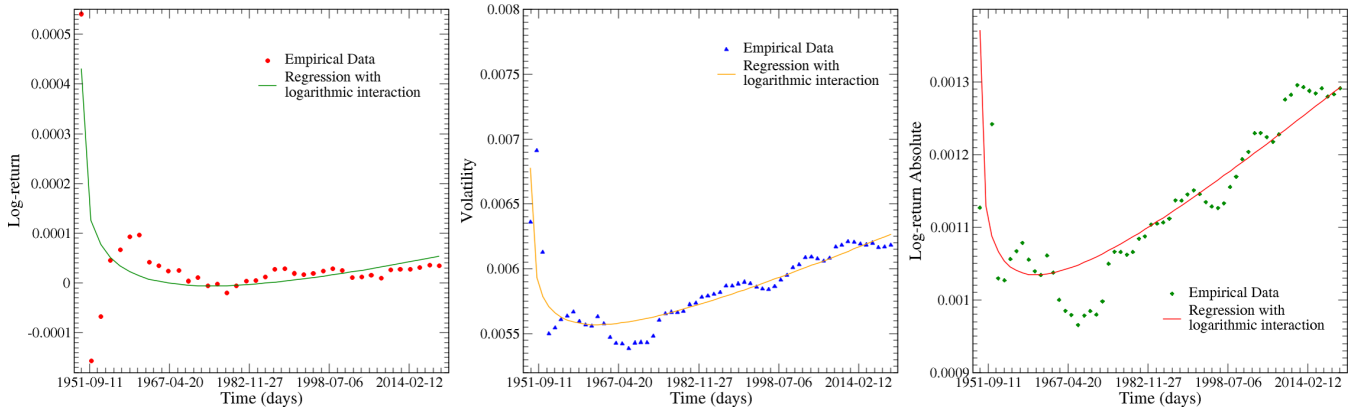

FIG. 5. Evolution of the mean of the time series of the S&P 500 stock index measured daily from January 3, 1950 to August 24, 2020 by scaling the data weekly (every five data) and taking the average of the total accumulated data each window size WS. Left: Log-return time series ($WS = 95$ data). Center: Volatility time series ($WS = 60$ data). Right: Log-return absolute time series ($WS = 60$ data).

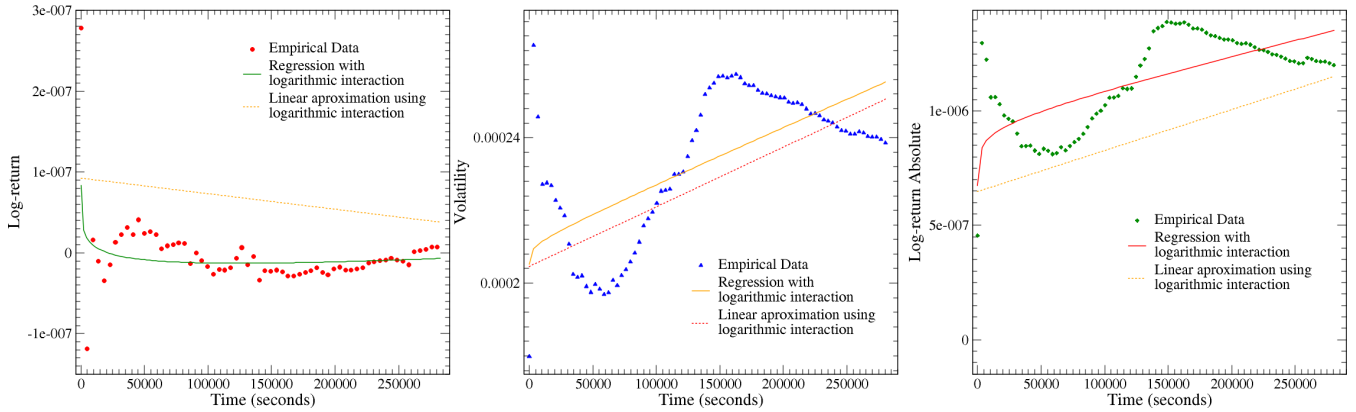

FIG. 6. Evolution of the mean of the time series of the Dow Jones stock index measured every 2 sec from October 10, 2014 at 09:30:03 to October 31, 2014 at 16:20:00 by scaling the data every 40 sec (every 20 data) and taking the average of the total accumulated data each window size WS. Left: Log-return time series ($WS = 113$ data). Center: Volatility time series ($WS = 173$ data). Right: Log-return absolute time series ($WS = 173$ data).

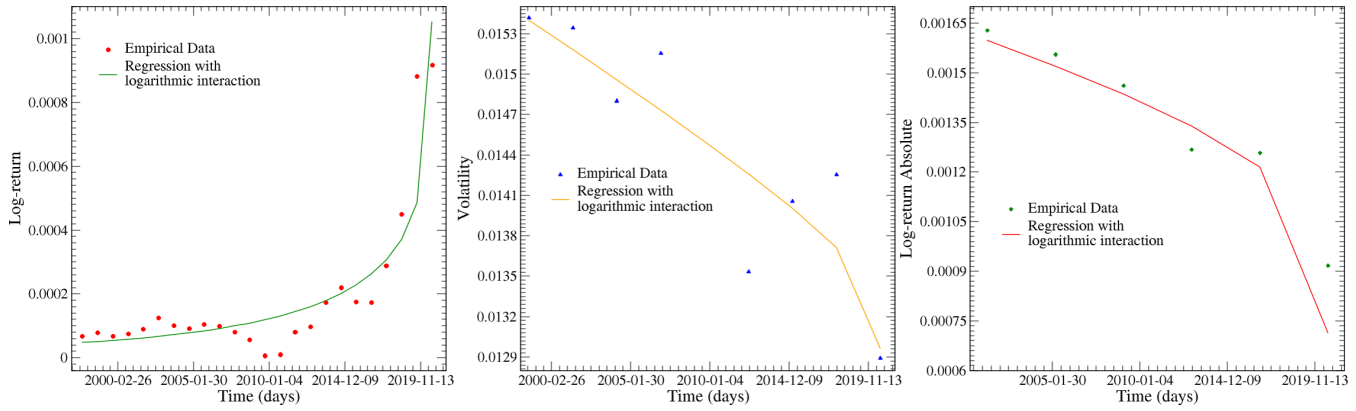

FIG. 7. Evolution of the mean of the time series of the FTSE stock index measured daily from October 20, 1997 to August 24, 2020 by scaling the data weekly (every five data) and taking the average of the total accumulated data each window size WS. Left: Log-return time series ($WS = 50$ data). Center: Volatility time series ($WS = 138$ data). Right: Log-return absolute time series ($WS = 194$ data).

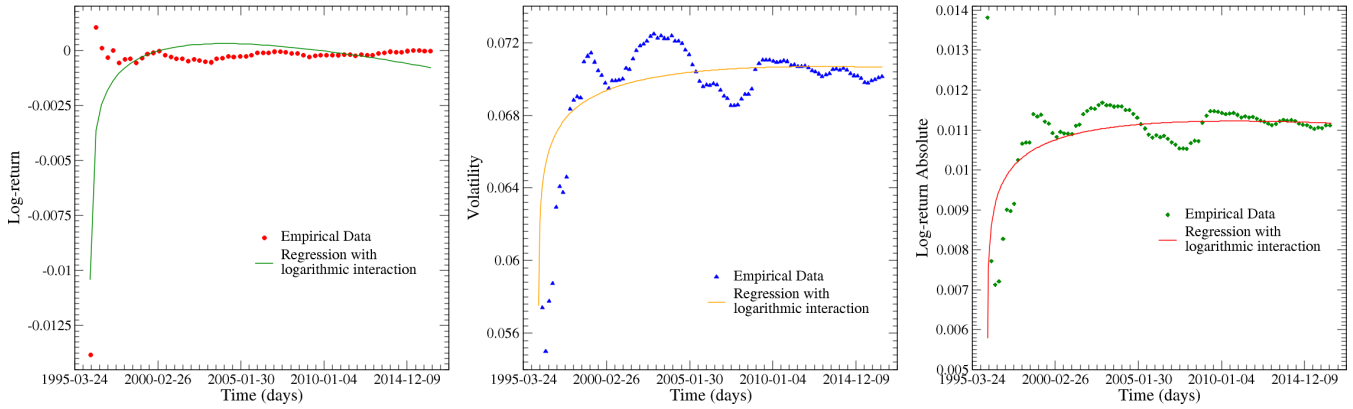

FIG. 8. Evolution of the mean of the time series of the Nikkei 225 stock index measured daily from January 4, 1984 to August 24, 2020 moving the time series in 3000 data (12 and a half years) and taking the average of the total accumulated data each window size WS. Left: Log-return time series ($WS = 84$ data). Center: Volatility time series ($WS = 17$ data). Right: Log-return absolute time series ($WS = 14$ data).

even at the high-frequency limit. However, for sufficiently large time values, the evolution of the average is seen in a linear fashion.

C. Evolution of time series temporarily moved

In this method with the scaling of the data of each time series, Figs. 8–11 are obtained for the Nikkei 225, S&P 500, Dow Jones, and FTSE stock index, respectively. It is observed that the regression with logarithmic term better adjusts the tendency of the empirical data and that in addition to comparing with the previous method the form of the regression curve prevails with (32), which implies that the adjustment with the logarithmic term it is invariant under temporal translations, which does not occur with the Kleinert model. Again, it is observed that the time series of log-return have a high GBE with a value of χ^2 less than 1. In addition, for the Dow Jones stock index it is observed that the adjustment improves as time passes, which implies that for the low-frequency limit the logarithmic term does not describe the total behavior of the nonstationary FTS.

D. Evolution of time series of other financial derivative

The previous sections allow us to conclude that the time series for stock indexes are invariant under scale and time translations under the adjustment with the logarithmic term. Thus and as proof that this adjustment can be applied to other types of financial derivatives, the regression is made for the time series of the currency of Colombian pesos to the U.S. dollar (COP-USD). Figure 12 is obtained for the COP-USD foreign exchange measured daily, and it is observed again that the regression with logarithmic term better adjusts the tendency of the empirical data and that in addition to comparing with the previous method the form of the regression curve prevails with the (32). It is important to mention that the regression data obtained for the drift r_x, cumulative c_1, and scale b parameters are in Table II. It is observed that the Kleinert linear model is not good for this type of financial derivatives and that it also does not reproduce the fact that the variance of the data can start from a nonzero value.

If x is a stochastic process such that its distribution function is stable [42], then we can conclude from the invariance under translations and time scaling of the mean that this will be a preserved property for all higher order moments since from

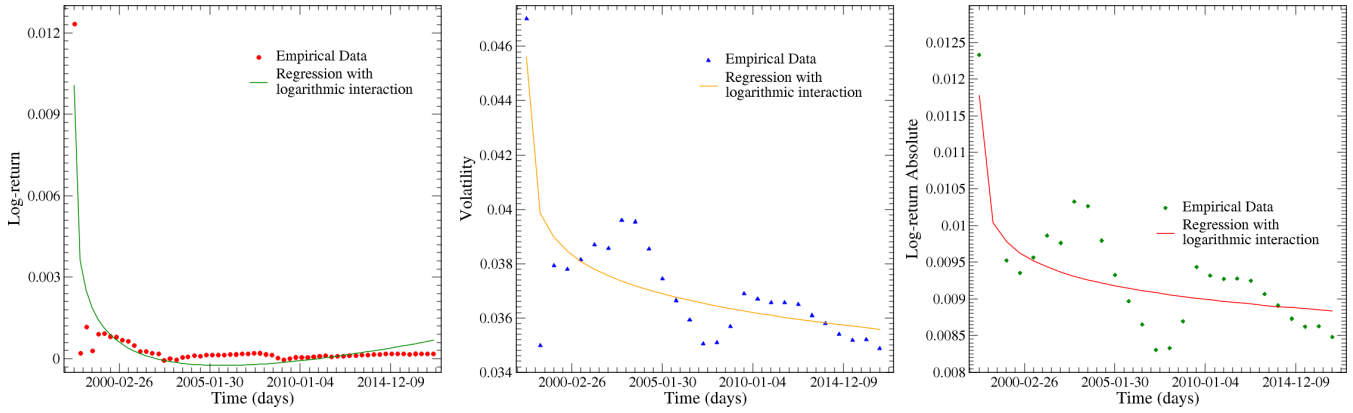

FIG. 9. Evolution of the mean of the time series of the S&P 500 stock index measured daily from January 3, 1950 to August 24, 2020 moving the time series in 12 000 data (50 yr) and taking the average of the total accumulated data each window size WS. Left: Log-return time series ($WS = 82$ data). Center: Volatility time series ($WS = 186$ data). Right: Log-return absolute time series ($WS = 186$ data).

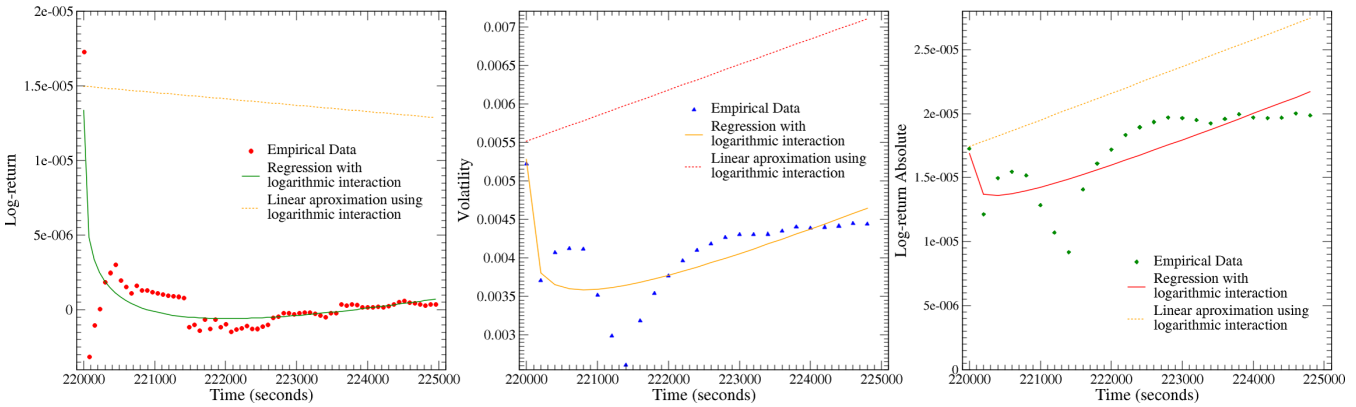

FIG. 10. Evolution of the mean of the time series of the Dow Jones stock index measured every 2 sec from October 10, 2014 at 09:30:03 to October 31, 2014 at 16:20:00 moving the time series in 220 000 data (8 days, 6 h, 26 min, and 40 sec) and taking the average of the total accumulated data each window size WS. Left: Log-return time series ($WS = 74$ data). Center: Volatility time series ($WS = 200$ data). Right: Log-return absolute time series ($WS = 200$ data).

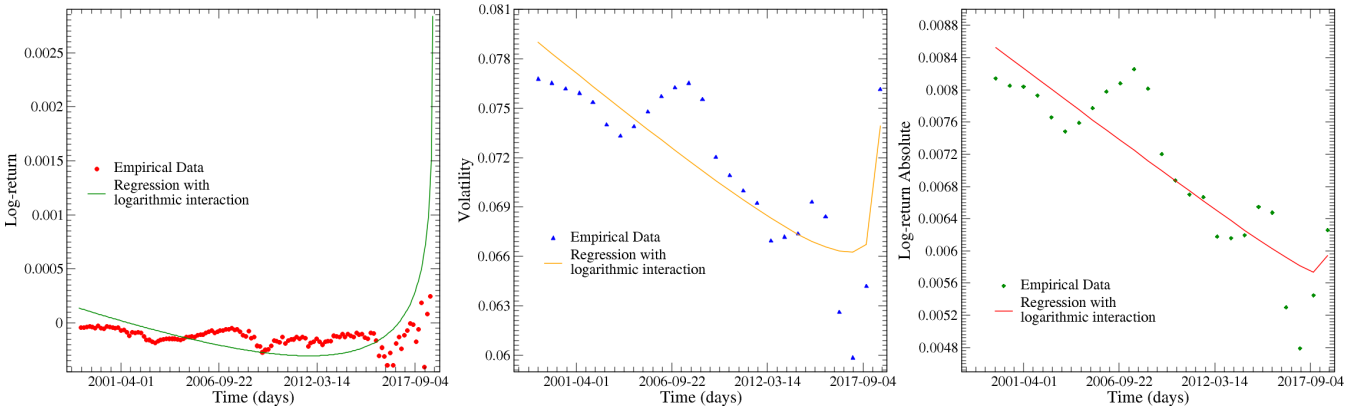

FIG. 11. Evolution of the mean of the time series of the FTSE stock index measured daily from October 20, 1997 to August 24, 2020 moving the time series in 500 data (2 yr) and taking the average of the total accumulated data each window size WS. Left: Log-return time series ($WS = 20$ data). Center: Volatility time series ($WS = 198$ data). Right: Log-return absolute time series ($WS = 200$ data).

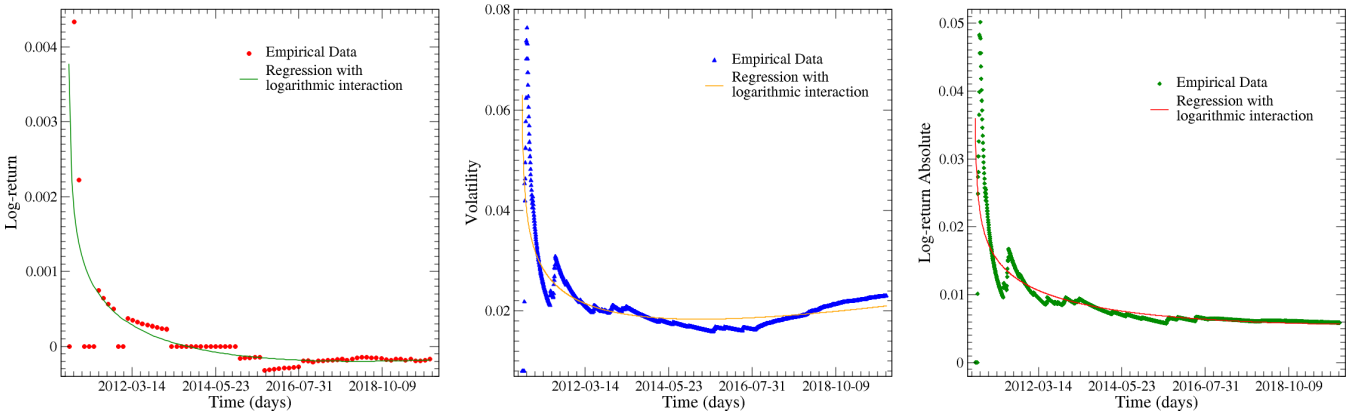

FIG. 12. Evolution of the mean of the time series of the COP-USD foreign exchange measured daily from July 16, 2010 to February 11, 2020 taking the average of the total accumulated data each window size WS. Left: Log-return time series ($WS = 20$ data). Center: Volatility time series ($WS = 30$ data). Right: Log-return absolute time series ($WS = 30$ data).

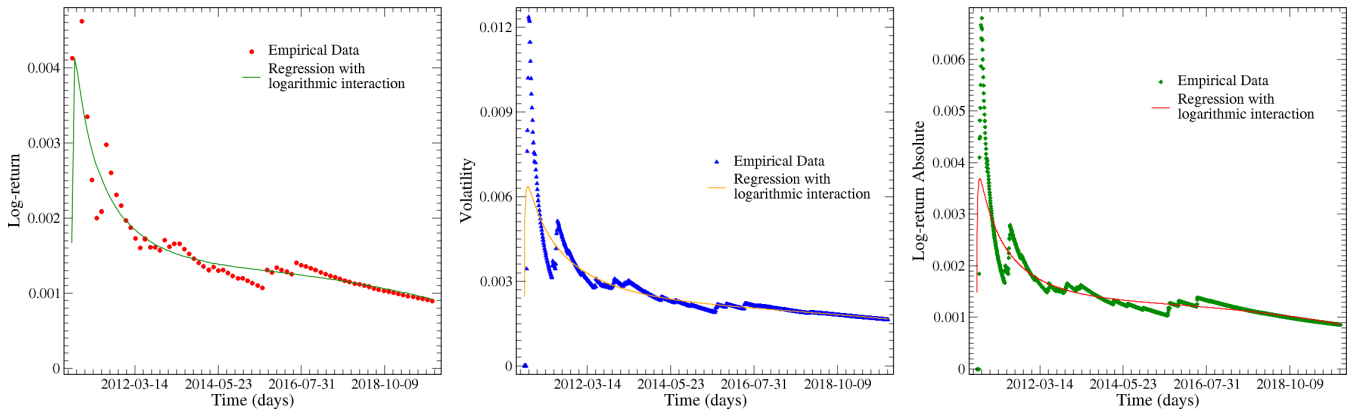

FIG. 13. Evolution of the variance of the time series of the COP-USD foreign exchange measured daily from July 16, 2010 to February 11, 2020 taking the variance of the total accumulated data each window size ($WS = 132$ data) for all time series. Left: Log-return time series. Center: Volatility time series. Right: Log-return absolute time series.

Eq. (32) we have

$$\begin{aligned}\Xi_n(t) &= \mathbb{E}[[x(t) - \Upsilon_1(t)]^n] \\ &= \mathbb{E}\left[\sum_{k=1}^{n}\binom{n}{k}(-1)^k x^{n-k}(t)\Upsilon_1^k(t)\right] \\ &= \sum_{k=1}^{n}\binom{n}{k}(-1)^k\Upsilon_1^k(t)\mathbb{E}[x^{n-k}(t)] \\ &= \sum_{k=1}^{n}\binom{n}{k}(-1)^k\Upsilon_1^k(t)\Upsilon_{n-k}(t).\end{aligned}$$

Then, under a related transformation $t \mapsto t' = \alpha t + \beta$, with $\alpha > 0$, $\beta \in \mathbb{R}$, we obtain $\Xi_n(t) \mapsto \Xi_n(t')$ where

$$\begin{aligned}\Xi_n(t') &= \sum_{k=1}^{n}\binom{n}{k}(-1)^k\Upsilon_1^k(t')\Upsilon_{n-k}(t') \\ &= \sum_{k=1}^{n}\binom{n}{k}(-1)^k\Upsilon_1^k(\alpha t+\beta)\Upsilon_{n-k}(\alpha t+\beta) \\ &= \sum_{k=1}^{n}\binom{n}{k}(-1)^k\Upsilon_1'^k(t)\Upsilon'_{n-k}(t). \qquad (44)\end{aligned}$$

Expression (44) indicates that moments such as variance preserve their functional form under scale and temporal translation transformations, and this is noted with primed indices that preserve the form of Eq. (32) but with different parameters. Thus, when analyzing the variance of the time series of the currency COP-USD with the three defined financial derivatives (37), (38), and (39), Fig. 13 is obtained. The regression data obtained for the drift r_x, cumulants c_1 and c_2, and scale b parameters are found in Table II. It is obtained that, unlike the stock indexes, the currency COP-USD has a GBE no greater than 8% and a χ^2 much less than 1, corroborating that the adjustments proposed with Eqs. (32) and (33) are valid.

An important result is the significant decrease in all three time series in Fig. 12, such that it shows the significant change in the price of the dollar with respect to the Colombian peso, as has occurred. In fact, if the error for each empirical data is taken from the weighted standard deviation [variance adjustment (33) weighted at each instant of time], Fig. 14 is obtained.

In Fig. 14 we show an extension in the tail of each financial series where the empirical data is contrasted with the extrapolation given by Eq. (32). This allows us to see that the quality of the adjustment in each time series is well described in the range defined by (32) with a deviation given by the weighting of (33) with the number of data in the time series N. For completeness, it is emphasized that to know the exact value of the conversion of the Colombian peso to the dollar, the value of the time series for a prior day is needed *a priori*, and then, for example, on March 12 of 2020, the series of the absolute log-return has $LA = (5.911991 \pm 0.17963) \times 10^{-3}$, which implies that the value of the Colombian peso with respect to the dollar $S(t)$ is

$$\begin{aligned}S(t) &= S_0 e^{LR} = 2.48 \times 10^{-4} e^{LR} \\ &= (2.49471 \pm 0.0334356) \times 10^{-4},\end{aligned}$$

where S_0 is the value of the time series the previous day, that is, from March 11, 2020. Therefore, one dollar is equivalent to $[(2.49471 \pm 0.0334356) \times 10^{-4}]^{-1} = 4008.49 \pm 54.45$ Colombian pesos, which compared to the value registered that day, which was 3977 Colombian pesos, there is a percentage error of $(0.7856 \pm 0.2415)\%$ with respect to our approach.

Repeating this calculation for the highest day in history (March 23, 2020), we have for the series of the absolute log-return $LA = (5.659726 \pm 0.15802) \times 10^{-3}$, $S_0 = 2.43 \times 10^{-4}$. Then one dollar is equivalent to $[(2.44379 \pm 0.0719122) \times 10^{-4}]^{-1} = 4092.0 \pm 124.1$ Colombian pesos, which compared to the value registered that day, which was 4176.5 Colombian pesos, there is a percentage error of $(2.065 \pm 1.127)\%$ with respect to our approach.

For comprehensiveness reasons and to see the modeling strength of this new approach, the evolution of the empirical data is calculated again up to August 24, 2020 illustrated in Fig. 15. Figure 15 shows the cumulative mean of the COP-USD currency as a function of time where an error in the non-normalized variance is assumed, that is, without dividing by the total data, and where the modeling with a logarithmic

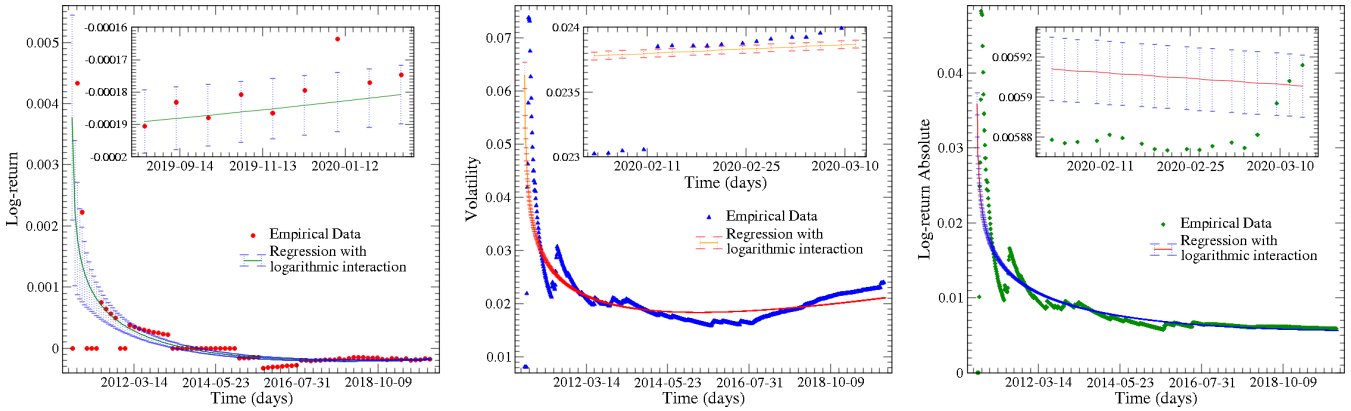

FIG. 14. Evolution of the mean of the time series of the COP-USD foreign exchange measured daily from July 16, 2010 to March 13, 2020 taking the mean of the total accumulated data keeping fixed the optimal window size found for each time series and taking the error in each data as the weight of the variance [found with the regression of Eq. (33)] when dividing by the total number of means N/WS. Left: Log-return time series ($WS = 20$ data). Center: Volatility time series ($WS = 30$ data). Right: Log-return absolute time series ($WS = 30$ data). The subcharts in each series represent an enlargement of the tail of the series used to observe the quality of the fit.

term (31) verifies that it is a more approximate model to describe the evolution in time of invariant nonstationary time series of temporal translations and scaling.

We conclude this section by highlighting that the variance of the currency data is expected to decrease over time since the time series of log-returns, volatilities, and absolute log-returns, constructed cumulatively, tend to a fixed value when increasing the number of data during long periods of stability in the market. Even so, from the monotonous increasing behavior for the FHT in a certain range of variances, it is worth studying the stability of this financial asset in the future, which is beyond the scope of this work.

VI. TEMPORAL EVOLUTION OF THE EXPONENT IN THE TFS FOR THE FTS

Figure 16 indicates the fit with empirical data of the variance as a function of the mean following TFS [Eq. (35)] for the time series of absolute log-returns for the currency COP-USD and for the volatilities time series of the stock index FTSE taking the size of the window in Tables III and V, respectively. These nonstationary time series satisfy the principle required for TFS where the time series is positive data. It is important to mention that from the adjustment we obtain $K = 0.1350 \pm 0.0052$ and $\alpha = 0.9465 \pm 0.0082$ with GBE of 5.77% for COP-USD absolute log-return time series, which implies that the evolution in time of this time series does not follow a linear relationship (although it is very close to being so) and whose exponent can be related to the scale parameter b [see Eq. (32) and Eq. (33)]. Observe that from Table II, the value of the cumulant c_1 and the value of the stochastic drift r_x are such that $c_1 t + r_x \ll 1$ for times small enough, which implies that the points scattered at the beginning of the figure are dominated by a quadratic behavior as stated by the expression (34). Furthermore, it is clear that if $\alpha < 1$ then $x^\alpha = O(x)$, which implies that asymptotically the variance behaves apparently linearly with respect to the mean of the time series, which is in agreement with expression (34). In the case of the volatility time series of the FTSE, we obtain $K = 0.2081 \pm 0.0054$ and $\alpha = 1.8901 \pm 0.0101$

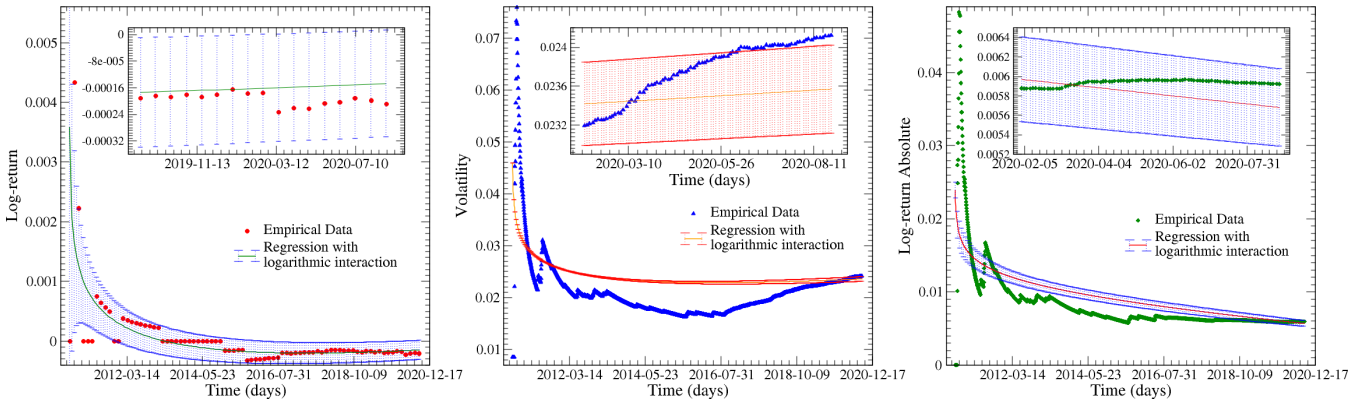

FIG. 15. Evolution of the mean of the time series of the COP-USD foreign exchange measured daily from July 16, 2010 to August 25, 2020 taking the mean of the total accumulated data keeping fixed the optimal window size found for each time series and taking the error in each data as the weight of the variance [found with the regression of Eq. (33)]. Left: Log-return time series ($WS = 20$ data). Center: Volatility time series ($WS = 30$ data). Right: Log-return absolute time series ($WS = 30$ data). The subcharts in each series represent an enlargement of the tail of the series used to observe the quality of the fit.

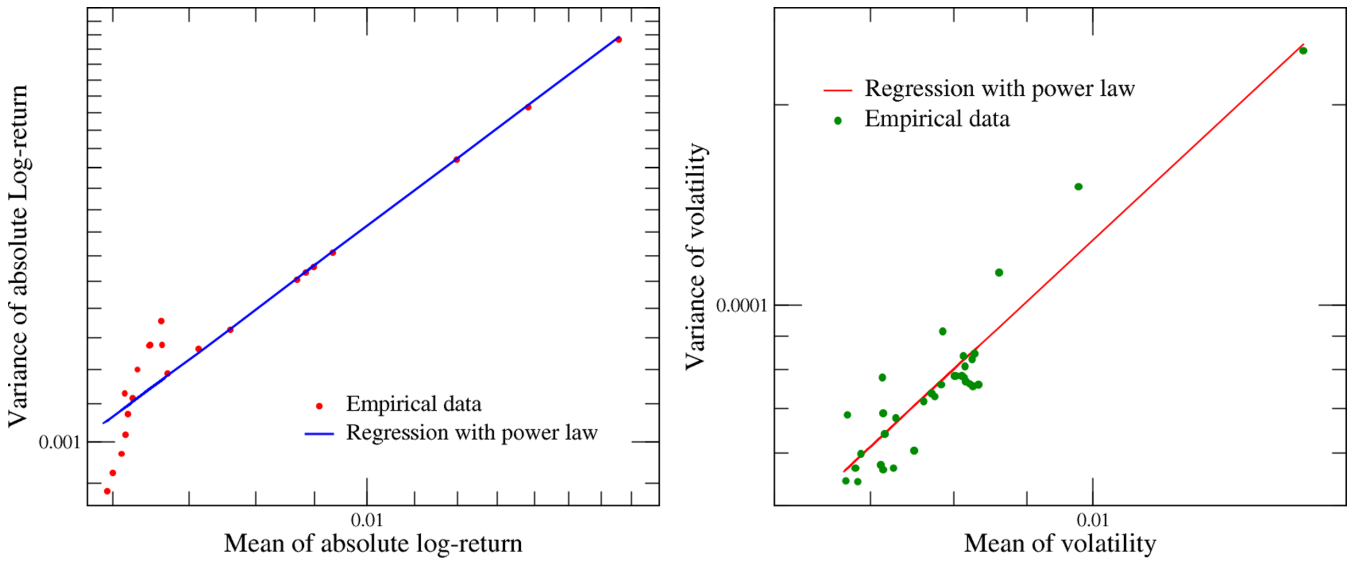

FIG. 16. Evolution of the variance of the time series as a function of the mean of the time series measured daily until August 24, 2020 taking the mean and variance of the total accumulated data, keeping the optimal window size fixed WS. (Left) Absolute log-return of COP-USD measured from July 16, 2010 with regression parameters $K = 0.1350 \pm 0.0052$, $\alpha = 0.9465 \pm 0.0082$ and GBE of 5.77% ($WS = 30$ data). (Right) Volatility of FTSE measured from October 20, 1997 with regression parameters $K = 0.2081 \pm 0.0054$, $\alpha = 1.8901 \pm 0.0101$, and GBE of 3.72% ($WS = 117$ data).

with GBE of 3.72%, this is a good fit observed for all the data with a exponent close to 2, indicating that the effect of the linear terminal at (34) is not strong enough to alter the usual variance relationship as a function of the square of the mean of the distribution. Thus, developing the adjustment of the time series of volatilities and absolute log-returns of the other financial assets, Table IV is obtained, which shows the adjustment parameters of the FS for each of the mentioned time series. It is important to note that the GBE (%) is no greater than 19%, and less than 10% in most cases, indicating a good approximation to the TFS for all financial assets.

Figure 17 shows the evolution of the TFS exponent $\alpha(t)$ for the absolute log-returns of the currency COP-USD and for the volatilities time series of the stock index FTSE taking the size of the window in Tables III and V, respectively. The adjustments were made taking into account Eq. (36) and the parameters already found for the cumulants, the stochastic drift, and the constant of the TFS shown in Tables III, IV, and V. The percentage errors of the time series of absolute log-returns of COP-USD and the time series of volatilities of FTSE were 2.8078% and 2.9408%, respectively, indicates that the mentioned evolution of TFS exponent in the expression (36) corresponds in a very good approximation to the behavior of the empirical data knowing only the initial cumulants of the distribution, the constant K, the scale parameter b, and the stochastic drift r_x. It is clear that as time increases, there is better precision in the value of the exponent, while initially this exponent easily fluctuates due to drastic changes in the mean or variance, which implies that asymptotically, the value of the exponent of the TFS tends to stabilize on a central value that would allow characterizing the type of financial derivative, or more generally, the type of time series that is being talked about. Finally, note that the empirical data were taken from the second time window where it makes sense to always be able to define the variance of the distribution without the problem of the normalization factor of the variance of a data sample proportional to $N - 1$.

VII. CONCLUSIONS

Taking as a starting point the model developed by Kleinert that uses the Feynman path integral to describe the evolution

TABLE III. Comparison of empirical data with the extrapolation of Eqs. (32) and (33) for the date mentioned in each time series. The regression with the new model refers to the one introduced in this article with the time-dependent logarithmic term, and the percentage error is calculated taking as a theoretical value the one given by Eq. (32).

	Moment	Empirical data	Regression new model	Error (%)
Log-return (February 21, 2020)	Mean	-1.7463×10^{-4}	-1.8080×10^{-4}	3.4083
	Variance	8.8690×10^{-4}	8.9889×10^{-4}	1.3341
Volatility (March 13, 2020)	Mean	2.4058×10^{-2}	2.3875×10^{-2}	0.76871
	Variance	1.6078×10^{-3}	1.6479×10^{-3}	2.4344
Absolute Log-return (March 13, 2020)	Mean	5.9159×10^{-3}	5.9055×10^{-3}	0.17663
	Variance	8.5194×10^{-4}	8.5932×10^{-4}	0.85847

TABLE IV. Adjustment parameters of the TFS in the time series of volatilities and absolute log-returns for the five financial assets studied.

Time series	K	α	Global error GBE (%)	χ^2
COP-USD Volatility	$(1.057 \pm 0.288) \times 10^{0}$	1.5317 ± 0.0777	14.83	9.106×10^{-4}
COP-USD Abs Log-return	$(1.350 \pm 0.052) \times 10^{-1}$	0.9465 ± 0.0082	5.77	1.948×10^{-4}
Nikkei 225 Volatility	$(2.449 \pm 0.086) \times 10^{-1}$	1.9751 ± 0.0127	4.32	2.006×10^{-4}
Nikkei 225 Abs Log-return	$(7.666 \pm 0.508) \times 10^{-2}$	1.4276 ± 0.0142	9.65	1.108×10^{-4}
S&P 500 Volatility	$(3.579 \pm 0.052) \times 10^{0}$	2.7534 ± 0.0041	2.61	3.898×10^{-5}
S&P 500 Abs Log-return	$(8.505 \pm 0.162) \times 10^{1}$	2.8516 ± 0.0037	5.13	2.368×10^{-5}
Dow Jones Volatility	$(4.972 \pm 1.796) \times 10^{-4}$	0.6902 ± 0.0656	15.66	1.666×10^{-5}
Dow Jones Abs Log-return	$(6.773 \pm 4.446) \times 10^{-2}$	1.6515 ± 0.0602	18.28	1.511×10^{-9}
FTSE 100 Volatility	$(2.081 \pm 0.054) \times 10^{-1}$	1.8901 ± 0.0101	3.72	2.174×10^{-4}
FTSE 100 Abs Log-return	$(1.314 \pm 0.079) \times 10^{0}$	2.0098 ± 0.0127	7.67	2.705×10^{-5}

in time of the moments of a probability distribution associated with log-returns, we extended this formalism for nonstationary time series, that is, time series with nonzero time correlation. The results are synthesized in (1) calculation of the functional relationship of the cumulants of a distribution of probability with incomplete Bell polynomials in Sec. II [44,45], (2) extension in the inclusion of nonzero stochastic drift in the temporal evolution of the probability distribution and in the temporal evolution of the central moments and around the origin of the distribution in Sec. III B [32,34], (3) study of the invariance of scale and temporal translations of the adjustment with the logarithmic term in the cumulant generating function (31) which allows us to establish a better correspondence between empirical data and the analytical evolution using the stochastic path integral (32) regardless of the frequency of the data, and this logarithmic term is defined by introducing a weight function in the calculation of the moments of the distribution (see Appendix C), and (4) obtaining the TFS that indicates the analytical evolution of the exponent of said law over time [see (36)], which in principle allows characterizing a time series and verifying the nonstationarity of FTS independently of the market and the chosen time interval.

It is also possible to speculate on the value of the financial derivative associated with the COP-USD foreign exchange with good precision and accuracy by extrapolating the values of Eq. (32) and taking as a deviation the weight of (33) with the data number N. It is important to mention that these results are applicable to any complex system that can be associated with a stochastic process with a causal structure, that is, all every nonstationary time series. In the future, it is expected to be able to extend this formalism at moments of noninteger orders for distributions that do not satisfy the central limit theorem [29]. In order to do this, we would like to see the generalization of TFS [1–3] with the Laskin path integral of fractional quantum mechanics [37] that introduces the Lévy distributions. Also, it is expected to study the regression of higher moments such as asymmetry and kurtosis that require more computational resources and nonlinear regression methods. In addition, we hope in the future to be able to analyze the relationship between the FHT and the variance of the financial assets studied in order to understand the region of stability in which each of the FTS is located with respect to the curve of nonmonotonous behavior between the FHT and the variance [22–24]. It is important to emphasize that Eq. (33) describes the variance as a deterministic variable, unlike other stochastic

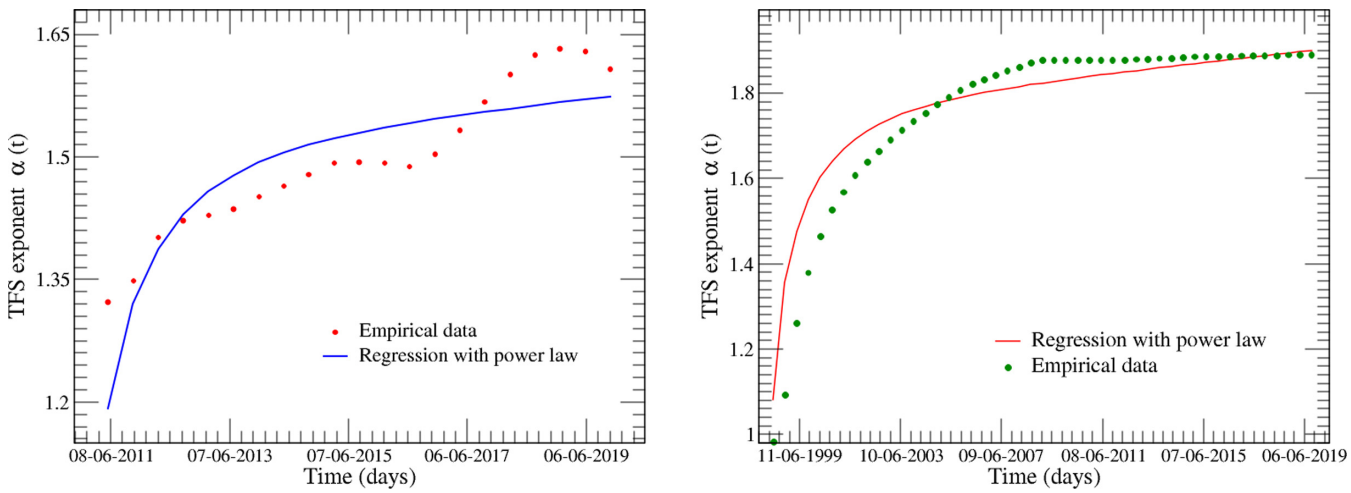

FIG. 17. Evolution of the TFS exponent as a function of the time measured daily until August 24, 2020 taking the mean and variance of the total accumulated data, keeping the optimal window size fixed WS. (Left) Absolute log-return of COP-USD measured from July 16, 2010 with regression parameters $K = 0.1350 \pm 0.0052$, $\alpha = 0.9465 \pm 0.0082$ and GBE of 5.77% ($WS = 30$ data). (Right) Volatility of FTSE measured from October 20, 1997 with regression parameters $K = 0.2081 \pm 0.0054$, $\alpha = 1.8901 \pm 0.0101$, and GBE of 3.72% ($WS = 117$ data).

models such as the GARCH model, the Heston model, and the nonlinear Heston model.

ACKNOWLEDGMENTS

We wish to acknowledge the support of the Physics Department of Universidad Nacional de Colombia.

F.S.A. and C.J.Q. conceptualized the work; F.S.A. carried out the codes for the adjustments.

APPENDIX A: MOMENTS AROUND THE ORIGIN, CENTRAL MOMENTS, AND CUMULANTS

The formula of Faà di Bruno for the nth derivative of the composition of functions is given by [46]

$$\frac{d^n}{dx^n}f(g(x)) = \sum_{\mathcal{N}} \frac{n!}{m_1!m_2!\cdots m_n!} f^{(m_1+m_2+\cdots+m_n)}(g(x)) \times \prod_{j=1}^{n}\left[\frac{g^j(x)}{j!}\right]^{m_j}, \tag{A1}$$

where

$$\mathcal{N} = \left\{(m_1, m_2, \ldots, m_n) \in \mathbb{N}_0^n \middle| \sum_{k=1}^{n} k\, m_k = n\right\}, \tag{A2}$$

or also, in terms of Bell's incomplete polynomials [44,45], the formula of Faà di Bruno has to be

$$\frac{d^n}{dx^n}f(g(x)) = \sum_{k=1}^{n} f^{(k)}(g(x))\mathcal{B}_{n,k}(g^{(1)}(x), \times g^{(2)}(x), \ldots, g^{(n-k+1)}(x)). \tag{A3}$$

Applying to the cumulant generating function with $f(p) = e^p$ and $g(p) = -H(p)$, it is

$$g^{(k)}(0) = -\left.\frac{d^k H(p)}{dp^k}\right|_{p=0} = (-i)^k c_k, \tag{A4}$$

$$f^{(k)}(p) = \frac{d^k}{dp^k}e^p = e^p, \quad \text{for all } k \in \mathbb{N}. \tag{A5}$$

Therefore, the moment nth centered around the origin using Eq. (5) is

$$\mu_n = i^n \sum_{k=1}^{n} e^{-H(0)}\mathcal{B}_{n,k}((-i)c_1, \ldots, (-i)^{n-k+1}c_{n-k+1}) = i^n \sum_{k=1}^{n} \mathcal{B}_{n,k}((-i)c_1, \ldots, (-i)^{n-k+1}c_{n-k+1}). \tag{A6}$$

The inverse relationship, that is, the cumulants in terms of the moments centered around the origin, is [43]

$$c_n = i^n \sum_{k=1}^{n}(-1)^{k-1}(k-1)! \times \mathcal{B}_{n,k}((-i)\mu_1, \ldots, (-i)^{n-k+1}\mu_{n-k+1}). \tag{A7}$$

It is important to highlight that the cumulants correspond to the nth central moment ξ_n, only for $n = 1, 2, 3$ denominated mean, variance, and skewness, respectively.

Generalizing for central moments, it has that the moments around the mean ξ_n and the cumulants c_n are related through [43]

$$\xi_n = i^n \sum_{k=1}^{n} \mathcal{B}_{n,k}(0, \ldots, (-i)^{n-k+1}c_{n-k+1}), \tag{A8}$$

$$c_n = i^n \sum_{k=1}^{n}(-1)^{k-1}(k-1)! \times \mathcal{B}_{n,k}(0, \ldots, (-i)^{n-k+1}\xi_{n-k+1}), \tag{A9}$$

and it is achieved by introducing the following minimal substitution into the cumulant generating function (analogous to Hamiltonian) $H(p) \mapsto H_{new}(p) = H(p) + i\mu_1 p$, where μ_1 is the first moment around the origin or expected value of the distribution.

APPENDIX B: EVOLUTION OF PROBABILITY DISTRIBUTION WITH NONZERO STOCHASTIC DRIFT

The probability that the system takes the value x_b in the time t_b since it had the value x_a in the time t_a through the probability distribution $\eta \equiv \eta(t)$ at a fixed time t, has a probability distribution given by $P_\eta(x_b, t_b|x_a, t_a) = \delta(x_\eta(t) - x_b)$ [34]. Taking into account all the contributions of the random variables $\eta(t)$ between the times t_a and t_b, it is obtained that the probability that the system reaches the value x_b at the time t_b given the value x_a at the time t_a is [34]

$$P(x_b, t_b|x_a, t_a) = \mathbb{E}_\eta[P_\eta(x_b, t_b|x_a, t_a)] = \int \mathcal{D}\eta P[\eta]\delta(x_\eta(t) - x_b), \tag{B1}$$

where $P[\eta]$ is a functional and $\mathcal{D}\eta$ is normalized by $\int \mathcal{D}\eta P[\eta] = 1$. Using the identity

$$\delta(x_\eta(t) - x_b) = \int_{x(t_a)=x_a}^{x(t_b)=x_b} \mathcal{D}x\delta[\dot{x} - \eta - r_x] = \int_{x(t_a)=x_a}^{x(t_b)=x_b} \mathcal{D}x \int_{-\infty}^{\infty} (\dot{x}(t) - \eta(t) - r_x)\delta(t)\, dt, \tag{B2}$$

we can conclude that the path integral to go from the value x_a in the time t_a to the value x_b in the time t_b is [34]

$$P(x_b, t_b|x_a, t_a) = \int_{x(t_a)}^{x(t_b)} \mathcal{D}x \int \mathcal{D}\eta P[\eta]\delta[\dot{x} - \eta - r_x], \tag{B3}$$

where the measure in the path integral over the stochastic variable $\mathcal{D}\mu = \mathcal{D}\eta\, P[\eta]$ in Eq. (B3) is called a *process measure* $\dot{x}(t) = r_x + \eta(t)$. Further, the path integral [34]

$$\int_{x(t_a)=x_a}^{x(t_b)=x_b} \mathcal{D}x\ \delta[\dot{x} - \eta - r_x], \tag{B4}$$

is called a *filter*, since it determines the value of the probability distribution x_b at the time t_b for all paths of $x(t)$ starting from x_a in time t_a following the equation of temporal evolution (18) expressed in the functional Dirac δ.

TABLE V. Regression data used to calculate the evolution of the mean over time for stock indexes Nikkei 225, S&P 500, Dow Jones, and FTSE 100 using the three filtering methods: Normal (all data), scaling (taking every n data) and translation (starting the series in the "Start" data and taking the 5000 consequent data).

Time series	Number of no null data	Filtration	Cumulant 1 regression c_1	Drift regression r_x	b	Drift theory r_x	Cumulant theory c_1	χ^2	Global error GBE (%)	Optimal window
Nikkei 225 Log-return	9011	Normal	-3.088×10^{-8}	1.722×10^{-3}	-1.661×10^{-4}	-1.367×10^{-4}	1.179×10^{-4}	1.357×10^{-2}	110.6	138
Nikkei 225 Volatility	9011	Normal	6.321×10^{-7}	2.590×10^{-2}	4.062×10^{-3}	5.354×10^{-2}	5.351×10^{-2}	3.677×10^{-3}	2.41	159
Nikkei 225 Abs Log-return	9011	Normal	2.259×10^{-7}	4.675×10^{-4}	9.058×10^{-4}	3.097×10^{-4}	6.300×10^{-3}	2.301×10^{-3}	5.91	159
Nikkei 225 Log-return	9011	Scaling weekly (5 days)	1.598×10^{-7}	6.701×10^{-4}	-1.348×10^{-4}	-8.971×10^{-5}	1.021×10^{-3}	8.523×10^{-3}	55.97	186
Nikkei 225 Volatility	9011	Scaling weekly (5 days)	8.448×10^{-7}	6.025×10^{-3}	8.352×10^{-4}	5.043×10^{-2}	5.023×10^{-2}	1.012×10^{-4}	2.25	159
Nikkei 225 Abs Log-return	9011	Scaling weekly (5 days)	2.734×10^{-7}	3.835×10^{-4}	1.745×10^{-4}	8.508×10^{-4}	4.913×10^{-3}	1.119×10^{-4}	5.30	125
Nikkei 225 Log-return	9011	Transfer of 3000 data	-9.261×10^{-7}	-1.166×10^{-2}	1.818×10^{-3}	1.209×10^{-4}	9.968×10^{-4}	5.743×10^{-2}	199.6	84
Nikkei 225 Volatility	9011	Transfer of 3000 data	-4.803×10^{-7}	5.618×10^{-2}	1.980×10^{-3}	6.212×10^{-2}	6.528×10^{-2}	3.425×10^{-2}	2.07	17
Nikkei 225 Abs Log-return	9011	Transfer of 3000 data	-2.325×10^{-7}	5.211×10^{-3}	8.365×10^{-4}	-1.905×10^{-3}	8.028×10^{-3}	2.190×10^{-2}	3.95	14
S&P 500 Log-return	17650	Normal	1.178×10^{-7}	6.805×10^{-3}	-8.499×10^{-4}	6.398×10^{-4}	6.289×10^{-4}	1.445×10^{-2}	66.37	171
S&P 500 Volatility	17650	Normal	4.360×10^{-7}	3.699×10^{-2}	-1.325×10^{-3}	2.690×10^{-2}	2.549×10^{-2}	2.256×10^{-3}	1.38	102
S&P 500 Abs Log-return	17650	Normal	1.702×10^{-7}	8.278×10^{-3}	-4.665×10^{-4}	1.147×10^{-3}	4.353×10^{-3}	1.534×10^{-3}	2.55	102
S&P 500 Log-return	17650	Scaling weekly (5 days)	6.270×10^{-8}	4.854×10^{-4}	-7.986×10^{-5}	4.542×10^{-5}	-7.817×10^{-4}	6.829×10^{-3}	151.9	95
S&P 500 Volatility	17650	Scaling weekly (5 days)	3.890×10^{-7}	6.951×10^{-3}	-2.523×10^{-4}	3.306×10^{-2}	3.358×10^{-2}	2.728×10^{-4}	1.47	60
S&P 500 Abs Log-return	17650	Scaling weekly (5 days)	1.316×10^{-7}	1.421×10^{-3}	-7.270×10^{-5}	-8.171×10^{-4}	7.951×10^{-3}	3.335×10^{-4}	3.30	60
S&P 500 Log-return	17650	Transfer of 12 000 data	8.515×10^{-7}	1.127×10^{-2}	-1.739×10^{-3}	1.977×10^{-4}	6.766×10^{-4}	2.602×10^{-2}	101.3	82
S&P 500 Volatility	17650	Transfer of 12 000 data	-3.328×10^{-8}	4.708×10^{-2}	-1.282×10^{-3}	3.648×10^{-2}	3.507×10^{-2}	1.308×10^{-3}	2.54	186
S&P 500 Abs Log-return	17650	Transfer of 12 000 data	7.877×10^{-9}	1.204×10^{-2}	-3.815×10^{-4}	1.055×10^{-3}	8.033×10^{-3}	1.018×10^{-3}	4.77	186
Dow Jones Log-return	240810	Scaling every 20 data (2s)	2.164×10^{-12}	9.250×10^{-8}	-1.360×10^{-8}	-3.316×10^{-8}	-5.593×10^{-6}	1.268×10^{-5}	232.6	113
Dow Jones Volatility	240810	Scaling every 20 data (2s)	3.035×10^{-9}	2.046×10^{-4}	8.508×10^{-7}	5.277×10^{-3}	5.286×10^{-3}	8.701×10^{-5}	5.55	173
Dow Jones Abs Log-return	240810	Scaling every 20 data (2s)	2.531×10^{-11}	6.481×10^{-7}	3.651×10^{-8}	-2.247×10^{-6}	2.587×10^{-5}	1.643×10^{-6}	11.13	173
Dow Jones Log-return	240810	Transfer of 220 000 data	1.167×10^{-9}	1.499×10^{-5}	-2.356×10^{-6}	-3.122×10^{-6}	-3.240×10^{-6}	2.006×10^{-4}	290.5	74
Dow Jones Volatility	240810	Transfer of 220 000 data	4.152×10^{-7}	5.517×10^{-3}	-3.382×10^{-4}	3.694×10^{-3}	3.697×10^{-3}	7.873×10^{-4}	6.51	200
Dow Jones Abs Log-return	240810	Transfer of 220 000 data	2.287×10^{-9}	1.742×10^{-5}	-7.899×10^{-7}	3.232×10^{-7}	1.215×10^{-5}	5.837×10^{-6}	9.42	200
FTSE 100 Log-return	5766	Normal	-5.310×10^{-7}	-9.326×10^{-3}	1.372×10^{-3}	6.398×10^{-4}	-1.455×10^{-3}	2.780×10^{-2}	53.30	146
FTSE 100 Volatility	5766	Normal	1.650×10^{-6}	9.708×10^{-2}	-3.500×10^{-3}	1.082×10^{-1}	1.104×10^{-1}	1.901×10^{-2}	1.08	117
FTSE 100 Abs Log-return	5766	Normal	2.289×10^{-7}	1.126×10^{-2}	-5.276×10^{-4}	-1.444×10^{-3}	1.407×10^{-2}	5.099×10^{-3}	1.56	172
FTSE 100 Log-return	5766	Scaling weekly (5 days)	9.735×10^{-8}	1.175×10^{-3}	-1.757×10^{-4}	4.502×10^{-4}	4.546×10^{-3}	8.196×10^{-4}	37.61	50
FTSE 100 Volatility	5766	Scaling weekly (5 days)	1.471×10^{-6}	1.288×10^{-2}	1.279×10^{-4}	7.257×10^{-2}	7.165×10^{-2}	7.865×10^{-5}	1.86	138
FTSE 100 Abs Log-return	5766	Scaling weekly (5 days)	4.409×10^{-7}	8.867×10^{-4}	4.652×10^{-5}	9.347×10^{-4}	6.325×10^{-3}	6.467×10^{-5}	7.20	194
FTSE 100 Log-return	5766	Transfer of 500 data	3.122×10^{-7}	3.215×10^{-3}	-5.443×10^{-4}	3.683×10^{-4}	-1.608×10^{-3}	9.135×10^{-2}	257.0	20
FTSE 100 Volatility	5766	Transfer of 500 data	3.749×10^{-6}	7.512×10^{-2}	-1.728×10^{-3}	6.393×10^{-2}	6.471×10^{-2}	2.324×10^{-3}	2.83	198
FTSE 100 Abs Log-return	5766	Transfer of 500 data	6.577×10^{-7}	5.994×10^{-3}	-7.411×10^{-5}	-3.506×10^{-4}	5.444×10^{-3}	8.016×10^{-4}	5.44	200

Taking $P[\eta] = \exp\{-\int_{t_a}^{t_b} dt \widetilde{H}[\eta(t)]\}$, where $\widetilde{H}$ is the logarithm of the chosen distribution $\widetilde{H}(\eta) = -\ln(\widetilde{D}[\eta])$, we conclude with the result in Eq. (19) [35,38].

APPENDIX C: MEAN AND VARIANCE WITH TIME-DEPENDENT LOGARITHMIC TERM

The deduction of Eq. (21) used that

$$\int_{-\infty}^{\infty} x^n e^{ipx}\, dx = 2\pi\ (-i)^n \frac{d^n}{dp^n}\delta(p), \tag{C1}$$

where the cumulant generating function (6) satisfies $H(0) = 0$.

Now, to introduce the logarithmic term (31) in the evolution of the mean and higher moments of the distribution, and the linear asymptotic linear behavior $[\Upsilon_1(t) = O(t)]$, we want to introduce a weight function $w(x)$ defined as

$$w(x) = 1 + \frac{b}{x}\ln(1+t). \tag{C2}$$

Then for the mean of distribution over the time we have

$$\Upsilon_1^{(H)}(t) = \int_{-\infty}^{\infty} \frac{dp}{2\pi} e^{-tH(p)-ipr_x} \int_{-\infty}^{\infty} dx\ x\ w(x) e^{ipx}\, dx$$
$$= \int_{-\infty}^{\infty} \frac{dp}{2\pi}\ e^{-tH(p)-ipr_x} \int_{-\infty}^{\infty} [x + b\ln(1+t)] e^{ipx}\, dx$$

TABLE VI. Markovian property test for stock indexes Nikkei 225, S&P 500, Dow Jones and FTSE and currency COP-USD. For the stock indexes, we use the 3 filtering methods: Normal (all data), scaling (taking every n data) and translation (starting the series in the "Start" data and taking the 5000 consequent data). For currency we take the mean and the variance data.

Index	Filtration	χ^2	Degrees of freedom	P value
Nikkei 225 Log-return	Normal	0.00000	65	1.0000
Nikkei 225 Volatility	Normal	0.00000	56	1.0000
Nikkei 225 Abs Log-return	Normal	0.00000	56	1.0000
Nikkei 225 Log-return	Scaling weekly (5 days)	0.00000	9	1.0000
Nikkei 225 Volatility	Scaling weekly (5 days)	0.00000	11	1.0000
Nikkei 225 Abs Log-return	Scaling weekly (5 days)	0.00000	14	1.0000
Nikkei 225 Log-return	Transfer of 3000 data	0.00000	59	1.0000
Nikkei 225 Volatility	Transfer of 3000 data	0.00000	294	1.0000
Nikkei 225 Abs Log-return	Transfer of 3000 data	0.00000	357	1.0000
S&P 500 Log-return	Normal	0.00000	103	1.0000
S&P 500 Volatility	Normal	0.00000	174	1.0000
S&P 500 Abs Log-return	Normal	0.00000	174	1.0000
S&P 500 Log-return	Scaling weekly (5 days)	0.00000	37	1.0000
S&P 500 Volatility	Scaling weekly (5 days)	0.00000	11	1.0000
S&P 500 Abs Log-return	Scaling weekly (5 days)	0.00000	59	1.0000
S&P 500 Log-return	Transfer of 12 000 data	0.00000	60	1.0000
S&P 500 Volatility	Transfer of 12 000 data	0.00000	26	1.0000
S&P 500 Abs Log-return	Transfer of 12 000 data	0.00000	26	1.0000
Dow Jones Log-return	Scaling every 20 data (2s)	0.00000	125	1.0000
Dow Jones Volatility	Scaling every 20 data (2s)	0.00000	81	1.0000
Dow Jones Abs Log-return	Scaling every 20 data (2s)	0.00000	81	1.0000
Dow Jones Log-return	Transfer of 220 000 data	0.00000	67	1.0000
Dow Jones Volatility	Transfer of 220 000 data	0.00000	24	1.0000
Dow Jones Abs Log-return	Transfer of 220 000 data	0.00000	24	1.0000
FTSE 100 Log-return	Normal	0.00000	39	1.0000
FTSE 100 Volatility	Normal	0.00000	49	1.0000
FTSE 100 Abs Log-return	Normal	0.00000	33	1.0000
FTSE 100 Log-return	Scaling weekly (5 days)	0.00000	23	1.0000
FTSE 100 Volatility	Scaling weekly (5 days)	0.00000	8	1.0000
FTSE 100 Abs Log-return	Scaling weekly (5 days)	0.00000	5	1.0000
FTSE 100 Log-return	Transfer of 500 data	0.00000	249	1.0000
FTSE 100 Volatility	Transfer of 500 data	0.00000	25	1.0000
FTSE 100 Abs Log-return	Transfer of 500 data	0.00000	24	1.0000
COP-USD Log-return	Mean	80.33929	112	0.9896
COP-USD Volatility	Mean	1.02041	1574	1.0000
COP-USD Abs Log-return	Mean	68.02041	1455	1.0000
COP-USD Log-return	Variance	0.00000	150	1.0000
COP-USD Volatility	Variance	0.02041	1489	1.0000
COP-USD Abs Log-return	Variance	0.02041	1489	1.0000

$$
\begin{aligned}
&= \int_{-\infty}^{\infty} dp\, e^{-tH(p)-ipr_x} \\
&\quad \times \left[-i\frac{d}{dp}\delta(p) + b\ln(1+t)\delta(p)\right] \\
&= i\frac{d}{dp}[e^{-tH(p)-ipr_x}]_{p=0} + b\ln(1+t) \\
&\quad \times [e^{-tH(p)-ipr_x}]_{p=0} \\
&= -i[tH'(0) + ir_x] + b\ln(1+t) \\
&= -i[ic_1 t + ir_x] + b\ln(1+t) \\
&= c_1 t + r_x + b\ln(1+t). \qquad \text{(C3)}
\end{aligned}
$$

Also

$$
\begin{aligned}
\Upsilon_2^{(H)}(t) &= \int_{-\infty}^{\infty} \frac{dp}{2\pi} e^{-tH(p)-ipr_x} \int_{-\infty}^{\infty} dx\, x^2\, w(x) e^{ipx}\, dx \\
&= \int_{-\infty}^{\infty} \frac{dp}{2\pi}\, e^{-tH(p)-ipr_x} \\
&\quad \times \int_{-\infty}^{\infty} [x^2 + bx\ln(1+t)] e^{ipx}\, dx \\
&= \int_{-\infty}^{\infty} dp\, e^{-tH(p)-ipr_x} \\
&\quad \times \left[(-i)^2 \frac{d^2}{dp^2}\delta(p) - ib\ln(1+t)\frac{d}{dp}\delta(p)\right]
\end{aligned}
$$

$$
\begin{aligned}
&= i^2 \frac{d^2}{dp^2}[e^{-tH(p)-ipr_x}]_{p=0} \\
&\quad + ib\ln(1+t)\frac{d}{dp}[e^{-tH(p)-ipr_x}]_{p=0} \\
&= tH''(0) - [H'(0)+ir_x]^2 - ib\ln(1+t) \\
&\quad \times [H'(0)+ir_x] \\
&= c_2 t - [ic_1 t + ir_x]^2 - ib\ln(1+t)[ic_1 t + ir_x] \\
&=, c_2 t + [c_1 t + r_x]^2 + b\ln(1+t)[c_1 t + r_x]. \quad \text{(C4)}
\end{aligned}
$$

Therefore, the variance as a function of time is

$$
\begin{aligned}
\Xi_2^{(H)} &= \Upsilon_2^{(H)}(t) - \left[\Upsilon_1^{(H)}(t)\right]^2 \\
&= c_2 t + [c_1 t + r_x]^2 + b\ln(1+t)[c_1 t + r_x] \\
&\quad - [c_1 t + r_x + b\ln(1+t)]^2 \\
&= c_2 t - (c_1 t + r_x) b\ln(1+t) - b^2 \ln^2(1+t). \quad \text{(C5)}
\end{aligned}
$$

It is important to note that with the interaction Hamiltonian (31) and Eq. (23), we obtain

$$
\begin{aligned}
\Upsilon_1^{(H)} &= \int_{-\infty}^{\infty} dx \frac{dp}{2\pi} x e^{-tH(p)+ip(x-r_x)-H_{\text{int}}(p,t)} \\
&= \int_{-\infty}^{\infty} dp\, e^{-tH(p)-ipr_x-H_{\text{int}}(p,t)}\left[-i\frac{d}{dp}\delta(p)\right] \\
&= i\frac{d}{dp}[e^{-tH(p)-ipr_x-H_{\text{int}}(p,t)}]_{p=0} \\
&= -i[tH'(0) + ir_x + ib\ln(1+t)] \\
&= c_1 t + r_x + b\ln(1+t), \quad \text{(C6)}
\end{aligned}
$$

which motivates the definition given to the time-dependent logarithmic term although it is important to mention that what is done is to introduce a new measure at the moments of the distribution with the weight function $w(x)$.

APPENDIX D: REGRESSION DATA

The theoretical regression data in Table V were taken with Kleinert's theory [35,36]. It is important to mention that these data should be divided by the interval between data (optimal window and scaling filter) in order to obtain a correct description of the evolution of the mean as shown in the Sec. V. Additionally, in the transferred time series, "Start" indicates from the data where the time series is taken.

APPENDIX E: MARKOV PROPERTY OF FTS

To establish the Markov property of the FTS, the *markovchain* package is used in the programming language R. In this package, the Markov property of a time series $(x_i)_{i=1}^N$ can be verified by setting a time instant t, with $1 \leqslant t \leqslant N-2$ and counting the number of times $n_{i,j,k}$ in which $x_t = i$, $x_{t+1} = j$ and $x_{t+2} = k$. Thus, n_{ijk} must follow a binomial distribution with parameters n_{ij} and p_{jk}. Finally, the χ^2 test is calculated on this distribution with q degrees of freedom in such a way that the P value is fixed with the inverse of the probability given by the right tail in the adjusted χ^2 test [55] (see Table VI).

[1] Z. Eisler, I. Bartos, and J. Kertész, Adv. Phys. **57**, 89 (2008).
[2] A. Fronczak and P. Fronczak, Phys. Rev. E **81**, 066112 (2010).
[3] J. E. Cohen and M. Xu, Proc. Natl. Acad. Sci. USA **112**, 7749 (2015).
[4] G. Blatter, M. V. Feigel'man, V. B. Geshkenbein, A. I. Larkin, and V. M. Vinokur, Rev. Mod. Phys. **66**, 1125 (1994).
[5] J. W. Kantelhardt, S. A. Zschiegner, E. Koscielny-Bunde, S. Havlin, A. Bunde, and H. E. Stanley, Physica A **316**, 87 (2002).
[6] B. Mandelbrot, Intl. Econ. Rev. **1**, 79 (1960).
[7] B. Mandelbrot, J. Bus. **36**, 394 (1963).
[8] S. H. Fairfield, J. Agri. Sci. **28**, 1 (1938).
[9] L. R. Taylor, Nature (London) **189**, 732 (1961).
[10] J. Kirchner, X. Feng, and C. Neal, Nature (London) **403**, 524 (1999).
[11] M. Tokeshi, Res. Popul. Ecol. **37**, 43 (1995).
[12] K. Linkenkaer-Hansen, V. V. Nikouline, J. M. Palva, and R. J. Ilmoniemi, J. Neurosci. **21**, 1370 (2001).
[13] G. Paladin and A. Vulpiani, Phys. Rep. **156**, 147 (1987).
[14] P. Gopikrishnan, V. Plerou, L. A. Nunes Amaral, M. Meyer, and H. E. Stanley, Phys. Rev. E **60**, 5305 (1999).
[15] V. Plerou and H. E. Stanley, Phys. Rev. E **76**, 046109 (2007).
[16] M. A. de Menezes and A. L. Barabási, Phys. Rev. Lett. **92**, 028701 (2004).
[17] P. C. Ivanov, A. Yuen, and P. Perakakis, PLoS ONE **9**, e92885 (2014).
[18] A. G. Zawadowski, J. Kertész, and G. Andor, Physica A **344**, 221 (2004).
[19] Z. Eisler and J. Kertész, Phys. Rev. E **73**, 046109 (2006).
[20] Z. Eisler, J. Kertész, S. H. Yook, and A. L. Barabási, Europhys. Lett. **69**, 664 (2005).
[21] L. Blanco, V. Arunachalam, and S. Dharmaraja, *Introduction to Probability and Stochastic Processes with Applications*, 3rd ed. (John Wiley & Sons, New York, 2012), Vol. 1.
[22] B. Spagnolo and D. Valenti, Int. J. Bifurcation Chaos Appl. Sci. Eng. **18**, 2775 (2008).
[23] D. Valenti, G. Fazio, and B. Spagnolo, Phys. Rev. E **97**, 062307 (2018).
[24] D. Valenti, B. Spagnolo, and G. Bonanno, J. Phys. A **382**, 311 (2007).
[25] G. Falci, A. L. Cognata, M. Berritta, A. D'Arrigo, E. Paladino, and B. Spagnolo, Phys. Rev. B **87**, 214515 (2013).
[26] G. Denaro, D. Valenti, A. L. Cognata, B. Spagnolo, A. Bonanno, G. Basilone, S. Mazzola, S. W. Zgozi, S. Aronica, and C. Brunet, Ecol. Complex. **13**, 21 (2013).
[27] N. Pizzolato, A. Fiasconaro, D. P. Adorno, and B. Spagnolo, Phys. Biol. **7**, 034001 (2010).
[28] A. Giuffrida, D. Valenti, G. Ziino, B. Spagnolo, and A. Panebianco, Eur. Food. Res. Technol. **228**, 767 (2008).
[29] V. Gnedenko and A. Kolmogorov, J. Math. Gaz. **39**, 342 (1955).
[30] S. Heston, Rev. Financ. Stud. **6**, 327 (1993).
[31] R. Cont and P. Tankov, *Financial Modelling with Jump Processes* (Chapman & Hall/CRC Press, Boca Raton, FL, London, 2004), Vol. 1.
[32] F. Black and M. Scholes, J. Polit. Econ. **81**, 637 (1973).

[33] R. Feynman, Rev. Mod. Phys. **20**, 367 (1948).
[34] H. Kleinert, in *Path Integrals in Quantum Mechanics, Statistics, Polymer Physics, and Financial Markets*, 5th ed. (Freie Universität Berlin, Germany, 1993), Vol. 1, pp. 1440–1535.
[35] H. Kleinert and X. J. Chen, Physica A **383**, 513 (2007).
[36] H. Kleinert, Physica A **311**, 536 (2002).
[37] N. Laskin, Phys. Lett. A **268**, 298 (2000).
[38] A. Issaka and I. SenGupta, J. Appl. Math. Comput. **54**, 159 (2016).
[39] K. Taufemback, R. Giglio, and S. D. Silva, Econ. Bull. **31**, 1631 (2011).
[40] H. M. Gupta and J. R. Campanha, Physica A **268**, 231 (1999).
[41] R. Friedrich, J. Peinke, M. Sahimi, and M. R. Rahimi, Phys. Rep. **506**, 87 (2011).
[42] R. LePage, K. Podgórski, and M. Ryznar, Probab. Theory Relat. Fields **108**, 281 (1997).
[43] M. Kendall and A. Stuart, *The Advanced Theory of Statistics*, 3rd ed. (Griffin, London, 1969), Sec. 3.12, Vol. 1.
[44] G. V. Voinov and M. S. Nikulin, Kybernetika **30**, 343 (1994).
[45] E. T. Bell, Ann. Math. **29**, 38 (1928).
[46] L. F. Arbogast, *Du calcul des derivations* (Levraut, Strasbourg, 1800), Chap. 1.
[47] R. Courant and D. Hilbert, *Chapter IV: The Calculus of Variations. Methods of Mathematical Physics* (Interscience Publishers, New York, 1953), Vol. 1.
[48] V. Popov, *Functional Integrals in Quantum Field Theory and Statistical Physics* (Springer-Verlag, Dordrecht, Netherlands, 1983).
[49] P. J. Daniell, Ann. Math. **20**, 281 (1919).
[50] A. Igorevich, *Mathematical Methods of Classical Mechanics*, 2nd ed. (Springer-Verlag, New York, 1989), Vol. 1.
[51] J. P. Sethna, *Statistical Mechanics. Entropy, Order Parameters and Complexity* (Laboratory of Atomic and Solid State Physics, Cornell, NY, 2006).
[52] B. Podobnik, D. Y. Horvatić, D. Kenett, and H. E. Stanley, Sci. Rep. **2**, 678 (2012).
[53] A. C. Silva and V. M. Yakovenko, Physica A **324**, 303 (2002).
[54] A. C. Silva, R. E. Prange, and V. M. Yakovenko, Physica A **344**, 227 (2004).
[55] G. A. Spedicato, The R Journal **9**, 84 (2017).